University of Alberta

Effects of Sphingomyelin Hydrolysis on Quantal Release from Rat Adrenal Chromaffin Cells

by

Jihuan Yin

A thesis submitted to the Faculty of Graduate Studies and Research
in partial fulfillment of the requirements for the degree of

Master of Science

Centre for Neuroscience

©Jihuan Yin
Fall, 2010
Edmonton, Alberta

Permission is hereby granted to the University of Alberta Libraries to reproduce single copies of this thesis and to lend or sell such copies for private, scholarly or scientific research purposes only. Where the thesis is converted to, or otherwise made available in digital form, the University of Alberta will advise potential users of the thesis of these terms.

The author reserves all other publication and other rights in association with the copyright in the thesis and, except as herein before provided, neither the thesis nor any substantial portion thereof may be printed or otherwise reproduced in any material form whatsoever without the author's prior written permission.

Examining Committee

Fredrick W. Tse and Amy Tse, Department of Pharmacology

Peter A. Smith, Department of Pharmacology

Glen B. Baker, Department of Psychiatry

Abstract

Sphingomyelin (SM), a sphingolipid that is concentrated in the extracellular leaflet of the plasma membrane, can interact with cholesterol to form more ordered "raft" domains. The hydrolysis of SM by sphingomyelinase (SMase) generates ceramide and may redistribute cholesterol molecules to other less ordered domains. I employed carbon fibre amperometry to examine whether SM hydrolysis affected the kinetics of release of catecholamines from individual granules of rat chromaffin cells when exocytosis was triggered by elevated extracellular [K^+]. Similar to cholesterol overload, SMase treatment selectively increased the proportion of "stand-alone foot" signals and the duration of the "pre-spike foot" signals; both effects could be reduced by extraction of cellular cholesterol. In contrast, the application of an exogenous ceramide did not mimic the effects of SMase. My results suggest that SMase treatment liberated cholesterol from lipid rafts to increase the persistence of the semi-stable fusion pore before the onset of rapid dilation.

Acknowledgements

I would like to thank my supervisors Drs. Fred and Amy Tse for their guidance and support, and Dr. Elena Posse De Chaves for her help in the lipid part of the research both theoretically and technically. Thanks also go to my supervisory committee members, Drs. Peter Smith and Glen B. Baker, for their suggestions and comments. Thank you to all the past and present members of the Tse lab including Dr. Nan Wang, Dr. Xiandi Gong, Dr. Andy K. Lee, Lei Yan and Valerie Yeung.

Table of contents

Chapter 1: General Introduction 1

I. Introduction 1

II. Chromaffin cell as a model for quantal release 2

III. Amperometry recordings 3

IV. Background on SM.....5

1. Metabolism of SM 5

2. Role of SM in signalling pathway 6

3. SM-cholesterol interaction.....7

V. Role of cholesterol in quantal release.....8

VI. My hypothesis.....9

References.....13

Chapter 2: Materials and Methods.....18

I. Chemicals and solutions 18

II. Cell Preparation.....18

III. Determination of cellular SM content.....19

IV. Determination of cellular cholesterol content 20

V. Measurement of $[Ca^{2+}]_i$ 21

VI. Electrical detection of catecholamine release.....22

VII. Data analysis.....23

References.....25

Chapter 3: Results 27

I. Change in cellular SM content with SMase treatment 27

II. Effects of SMase on quantal release.....27

III. The effects of SMase on quantal release mimics those of cholesterol overload29

IV. The effects of SMase on quantal release can be reduced by cholesterol extraction.....30

1. The effect of SMase (1U for 1hr) can be eliminated by cholesterol extraction.....30

2. The effects of SMase (0.1U overnight) can be partially reduced by cholesterol extraction and inhibition of cholesterol synthesis 31

V. The effects of SMase on quantal release cannot be mimicked by exogenous C6 ceramide overload.....33

VI. Change in detected cellular cholesterol content with SMase treatment 35

VII. Change in the depolarization-evoked Ca^{2+} signal with SMase treatment and cholesterol overload.....36

References.....56

Chapter 4: Discussion 57

I. Why did SMase treatment lead to a very modest drop in cellular SM content? 58

II. What are the possible mechanisms underlying the effects of SMase on quantal release kinetics? 59

III. What is the contribution of ceramide to the change in quantal release?.....63

IV. What is the contribution of a change in the triggering [Ca^{2+}] to the change in quantal release? 65

V. Physiological significance 66

VI. Conclusions.....67

VII. Future directions.....68

References.....71

List of figures

Figure 1.1 Scheme of amperometric recording from a chromaffin cell.....10

Figure 1.2 Examples of amperometric signals recorded from a rat adrenal chromaffin cell during the exocytosis of a LDCG.....11

Figure 1.3 Interaction between sphingomyelin (SM) and cholesterol and liberation of cholesterol after hydrolysis of SM from a lipid raft 12

Figure 3.1 Effects of SMase on cellular SM content 38

Figure 3.2 Effects of SMase (1U for 1hr or 0.1U overnight) on the number of events per cell, the proportion of "stand-alone foot" signals, the Q of the LDCGs (indicated by $Q^{1/3}$), and the proportion of events with a foot.....39

Figure 3.3 SMase did not affect the different kinetic parameters of the spike 40

Figure 3.4 SMase increased the foot duration, the foot area and the fractional release during foot.....41

Figure 3.5 Effects of SMase (1U for 1hr), cholesterol (0.1mg/ml for 1hr) and 1hr treatment of SMase (1U)+cholesterol (0.1mg/ml) on the number of events per cell, the proportion of "stand-alone foot" signals, the Q of the LDCGs, and the proportion of events with a foot.....42

Figure 3.6 SMase (1U for 1hr), cholesterol (0.1mg/ml for 1hr) and 1hr treatment of SMase (1U)+cholesterol (0.1mg/ml) did not affect the different kinetic parameters of the spike 43

Figure 3.7 SMase (1U for 1hr), cholesterol (0.1mg/ml for 1hr) and 1hr treatment of SMase (1U)+cholesterol (0.1mg/ml) increased the foot duration, the foot area and the fractional release during foot.....44

Figure 3.8 Effects of SMase (1U for 1hr), MβCD (5mM for 1hr) and 1hr treatment of SMase (1U)+MβCD (5mM) on the number of events per cell, the

proportion of “stand-alone foot” signals, the Q of the LDCGs, and the proportion of events with a foot 45

Figure 3.9 SMase (1U for 1hr), MβCD (5mM for 1hr) and 1hr treatment with SMase (1U)+MβCD (5mM) did not affect the different kinetic parameters of the spike 46

Figure 3.10 Effects of SMase (1U for 1hr), MβCD (5mM for 1hr) and 1hr treatment of SMase (1U)+MβCD (5mM) on the foot duration, the foot area and the fractional release during foot 47

Figure 3.11 Effects of SMase (0.1U overnight) and SMase+MβCD+lovastatin (5μM lovastatin and 0.1U SMase overnight prior to 5mM MβCD for 1hr) on the number of events per cell, the proportion of “stand-alone foot” signals, the Q of the LDCGs, and the proportion of events with a foot 48

Figure 3.12 SMase (0.1U overnight) and SMase+MβCD+lovastatin (5μM lovastatin and 0.1U SMase overnight prior to 5mM MβCD for 1hr) did not affect the different kinetic parameters of the spike 49

Figure 3.13 Effects of SMase (0.1U overnight) and SMase+MβCD+lovastatin (5μM lovastatin and 0.1U SMase overnight prior to 5mM MβCD for 1hr) on the foot duration, the foot area and the fractional release during foot 50

Figure 3.14 Effects of C6 ceramide (5μM for 1hr) and DMSO (0.1% for 1hr) on the number of events per cell, the proportion of “stand-alone foot” signals, the Q of the LDCGs, and the proportion of events with a foot 51

Figure 3.15 C6 ceramide (5μM for 1hr) and DMSO (0.1% for 1hr) did not affect the different kinetic parameters of the spike at matched values of $Q^{1/3}$ 52

Figure 3.16 Effects of C6 ceramide (5μM for 1hr) and DMSO (0.1% for 1hr) on the foot duration, the foot area and the fractional release during foot 53

Figure 3.17 Effects of SMase (1U for 1hr) and SMase (0.1U overnight) on cellular less organized cholesterol content in rat chromaffin cells 54

Figure 3.18 Effects of SMase (1U for 1hr), SMase (0.1U overnight) and cholesterol overload on the changes in $[Ca^{2+}]_i$.....55

Figure 4.1 Structure of the fusion pore 69

Figure 4.2 Comparison between C6 ceramide and C16 ceramide in their contribution to the lipid monolayer curvature.....70

List of abbreviations and symbols

AC: adenylyl cyclase

aSMase: acid Smase

ATP: adenosine 5'-triphosphate

BCA: bicinchoninic acid

cAMP: cyclic adenosine 3',5'-monophosphate

CERT: ceramide transfer protein

$[Ca^{2+}]_i$: cytosolic free calcium concentration

$\Delta[Ca^{2+}]_i$: change in cytosolic free calcium concentration

DAG: diacylglycerol

DAOS: N-ethyl-N-(2-hydroxy-3-sulfopropyl)-3, 5-dimethoxyaniline, sodium salt

DMSO: dimethyl sulfoxide

ER: endoplasmic reticulum

ITS: insulin-transferrin-selenium-A

LDCGs: large dense core granules

MβCD: methyl-β-cyclodextrin

nSMase: neutral, Mg^{2+}-dependent SMase

PBS: phosphate-buffered saline

pC: pico coulomb

PKC: protein kinase C

Q: quantal size

RIPA buffer: radioimmunoprecipitation assay buffer

SM: sphingomyelin

SMase: sphingomyelinase

SMS: SM synthase

SNAREs: soluble N-ethylmaleimide attachment protein receptors

sSMase: secretory SMase

τ: time constant

TNFα: tumor necrosis factor-α

VGCCs: voltage-gated calcium channels

Chapter 1: General Introduction

I. Introduction

Exocytosis is a vital process mediating the release of hormones or neurotransmitters from intracellular granules or vesicles through orderly execution of membrane fusion. In the last two decades, with the identification of various proteins that mediate regulated exocytosis, such as the SNAREs (soluble N-ethylmaleimide attachment protein receptors), significant progress has been made in the understanding of the role of proteins in regulating the molecular machinery of membrane fusion (Jackson & Chapman 2006, Jackson & Chapman 2008). In contrast, less is known about the roles of lipid molecules that comprise up to 50% of the mass of most mammalian cell membranes (Alberts *et al.* 1994). Lipid has long been regarded as a passive component during fusion and the release process. However, recently there is increasing evidence that lipids have important roles in secretion (Davletov *et al.* 2007, Lucic *et al.* 2007, Tang *et al.* 2007, Uchiyama *et al.* 2007, Vitale *et al.* 2001). Most importantly, the proper clustering of SNAREs was reported to be dependent on lipid domains that had been termed "rafts" (Lang *et al.* 2001b).

Lipid rafts are conventionally defined as detergent-resistant sphingolipid-cholesterol rich microdomains of the cell membrane (Simons & Ikonen 1997). Such ordered lipid domains have the ability to sequester specific proteins, thereby playing an important role in facilitating cellular processes and signal transduction. SNAREs are suggested to cluster in cholesterol-dependent membrane domains, although it is unclear whether these domains are indeed conventional lipid rafts (Lang 2007). Nevertheless, the extraction of cholesterol with methyl-β-cyclodextrin was reported to disrupt excitation-secretion coupling at a crustacean neuromuscular preparation (Zamir & Charlton 2006), the balance between evoked and spontaneous synaptic vesicle recycling in hippocampal neurons (Wasser *et al.* 2007), as

well as the Ca^{2+}-dependent fusion of sea urchin cortical granules (Churchward *et al.* 2005). Our lab has been studying the role of lipids in mediating and regulating exocytosis in rat adrenal chromaffin cells. A recent study in our lab has shown that cholesterol in the cytoplasmic leaflet of cellular membranes stabilizes the fusion pore of large dense core granules before the onset of rapid dilation (Wang *et al.* 2010). Here I have examined the role of another important lipid, sphingomyelin (SM), which can interact tightly with cholesterol in the plasma membrane in the quantal release process.

II. Chromaffin cell as a model for quantal release

Adrenal chromaffin cells are secretory cells located in the neuroendocrine part (medulla) of the adrenal gland. During embryonic development, some cells from the sympathetic promodium migrate from the neural crest to form the adrenal medulla (Tuchmann *et al.* 1972). Due to their embryonic derivation, chromaffin cells in the adrenal medulla have some neuronal characteristics. They synthesize and secrete catecholamines, mainly adrenaline and/or nonadrenaline, in response to stimulation by acetycholine released from the preganglionic sympathetic nerve fibres of the splanchnic nerve (Edwards & Jones 1993). Each bovine chromaffin cell contains ~21,000 granules (Plattner *et al.* 1997) with a mean vesicular diameter of ~200 nm. Because granules in chromaffin cells are larger than the synaptic vesicles (mean diameter of ~50 nm) in neurons and the lumen of each chromaffin granule contains an electron dense “core”, chromaffin granules are called large dense core granules (LDCGs). In individual LDCGs, 0.7-0.9 M of catecholamines are packaged along with a protein, chromogranin A, to form a gel-like matrix (Albillos *et al.* 1997, Wightman *et al.* 2002, Borges *et al.* 2000). This allows the storage of large amounts of catecholamines in individual granules without creating hyperosmolarity. The condensed material in the granule matrix leads to the appearance of a “dense core” image in electron micrographs (Koval *et al.* 2001). During the exocytosis of a single LDCG, ~7

million molecules of catecholamine are released into the circulation (Rahamimoff & Fernandez 1997, Albillos et al. 1997). The massive secretion of catecholamines regulates a variety of physiological functions, including the increase in heart rate and blood pressure during the "fight or flight" response (Fox 2004).

Chromaffin cells are widely used as a model to examine the kinetics of quantal release for the following reasons. Firstly, as described above, chromaffin cells and sympathetic neurons share a common embryonic origin. They share some common mechanisms in the synthesis of catecholamines and the triggering of exocytosis. Secondly, the amount of catecholamines secreted from each LDCG can be detected electrochemically with amperometry whose high sensitivity and temporal resolution allow one to monitor fusion kinetics (see below). Thirdly, the large pool of LDCGs in chromaffin cells (Plattner et al. 1997) allows many (typically ~100) amperometric signals to be recorded from each individual cell. Lastly, in comparison to neurons from which the majority of the transmitter release occurs at synapses located in axonal varicosities (Zhou & Misler 1995b) or terminals (Bruns *et al.* 2000) which are not easily accessible, robust exocytosis can occur over most of each chromaffin cell's surface (Fox 1996, Zhou & Misler 1995a, Robinson *et al.* 1995). Thus, amperometric signals can be more easily recorded from the cell surface of chromaffin cells.

III. Amperometry recordings

An important technique employed in the study of the kinetics of quantal release is carbon fibre amperometry (Chow & von Ruden 1995, Mosharov & Sulzer 2005). It is based on the sensitive detection of readily oxidized substances such as catecholamines by a carbon fibre electrode which is positioned to gently touch a chromaffin cell (Fig. 1.1). Upon simulation by high extracellular [K^+], the chromaffin cell is depolarized, leading to the activation of voltage-gated calcium channels (VGCCs). The influx of Ca^{2+}

through VGCCs triggers exocytosis, which results in the discharge of catecholamines from individual LDCGs. When a molecule of catecholamine reaches the surface of the carbon fibre electrode that is voltage clamped at +700 mV, it is oxidized and generates 2 electrons (detected as current by a conventional voltage-clamp amplifier). If the rate of exocytosis is modest, the amperometric signals from individual granules can be resolved. This high-resolution allows one to study the quantal release process.

When a granule undergoes exocytosis at the plasma membrane, the lumen of the granule initially forms a connection with the extracellular environment via a structure called the fusion pore (Fig. 1.2 A). Frequently the fusion pore first opens to a semi-stable state with a pore conductance typically < 0.5 nS (Albillos et al. 1997, Gong *et al.* 2007) and results in a leakage of catecholamines, giving rise to a foot signal. Usually, the decondensation of the granule matrix generates forces to overcome those initially constraining the size of semi-stable fusion pore such that it proceeds to rapid dilation. The rapid release of catecholamines via the dilated fusion pore gives rise to the spike phase of the amperometric signal. Sometimes, the semi-stable state of the fusion pore is too short such that no foot signal is detectable. This gives rise to an amperometric spike without a foot signal (Fig. 1.2 B). Occasionally, some fusion pores flicker and close before any significant dilation, giving rise to “stand-alone foot” signals (Fig. 1.2 C).

Fig. 1.2 A also shows some common parameters which are used to quantify the kinetics of the amperometric signal. These include: foot duration (the time interval of the foot signal, which reflects the stability of a fusion pore); foot amplitude (the amplitude at the end of the foot signal, which reflects the size of the fusion pore before rapid dilation); spike amplitude (the height of amperometric signal); 50-90% rise time (the time between 50 and 90% of the spike amplitude, which is an index of how rapidly the amperometric signal is rising); half-width (the time duration when the amperometric signal is above 50% of the spike amplitude); decay τ (the time constant of an

exponential fitted to the decay phase of the signal); quantal size (Q) which is the time integral of the signal, from which one can calculate the number of catecholamine molecules released per LDCG. The value of $Q^{1/3}$ is employed in some analyses of this study because the vesicular diameter of LDCGs was reported to have a Gaussian distribution (Albillos *et al.* 1997). If the concentration of catecholamine is assumed to be identical among the LDCGs (Gong *et al.* 2003), the distribution of values of $Q^{1/3}$ reflects the distribution of vesicular diameter.

IV. Background on SM

1. Metabolism of SM

SM is an essential lipid component of the plasma membrane in mammalian cells. Almost all SM of the plasma membrane is located in the extracellular leaflet; for example, 80–85% of the SM of human red cells is found in the exoleaflet (Barenholz & Thompson 1980, Verkleij *et al.* 1973). The precursor of SM is ceramide that is synthesized in the cytosolic leaflet of the endoplasmic reticulum (ER). Ceramide is then transported to the Golgi apparatus by the ceramide transfer protein (CERT) via the cytosol. At the Golgi apparatus, ceramide is translocated to the luminal leaflet (probably via spontaneous flip-flop) where SM is synthesized by the transfer of a phosphocholine moiety from phosphatidylcholine to ceramide, yielding diacylglycerol (DAG) as a side product. This process is catalyzed by SM synthase (SMS) (Bartke & Hannun 2009, Futerman & Riezman 2005). By means of vesicle budding, the synthesized SM in the luminal leaflet leaves the Golgi apparatus for the plasma membrane. When such vesicles fuse with the plasma membrane, SM becomes a part of the extracellular leaflet (van Meer & Holthuis 2000). So far two SMSs have been identified; both are transmembrane proteins. SMS1 is found mainly in the Golgi apparatus and is postulated to be responsible for the synthesis of the bulk of cellular SM. SMS2 was shown to primarily reside in the plasma membrane and is presumably

responsible for the production of SM in the plasma membrane (Huitema *et al.* 2004). Components in the plasma membrane are frequently internalized via endocytosis to be degraded or recycled. In this way, the majority of SM in the plasma membrane is trafficked via endocytosed vesicles to acidic compartments such as endosomes. Upon maturation, the endosome fuses with lysosomes, where SM is finally degraded by sphingomyelinase (SMase) to generate ceramide and phosphocholine (Ferlinz *et al.* 1999). In addition to the lysosome-associated degradation, SM can also be hydrolyzed in the plasma membrane by another type of SMase (see below). In recent years, this pathway of SM hydrolysis has been exploited in the study of the role of SM and ceramide in cellular signal transduction.

2. Role of SM in signalling pathway

The SMase-dependent SM-ceramide signalling pathway has been investigated extensively. At least five types of SMase have been identified (Goni & Alonso 2002): acid SMase (aSMase), secretory SMase (sSMase), neutral, Mg^{2+}-dependent SMase (nSMase), Mg^{2+}-independent neutral SMase and alkaline SMase (isolated from the intestinal tract). The best characterized SMases are the aSMase and nSMase. The aSMase is mainly located in lysosomes and its deficiency can result in Niemann-Pick disease, in which the accumulation of SM causes a variety of neurological disorders (Kolodny 2000, Schuchman 2007). It has been suggested that stress stimuli, such as ultraviolet radiation, chemotherapeutic agents and the potential anti-tumor agent apoptin, can trigger a translocation of aSMase to the extracellular leaflet of the plasma membrane, resulting in the cleavage of SM into ceramide (Liu *et al.* 2006, Schenck *et al.* 2007). The nSMase is a plasma membrane-associated enzyme and can be activated by various stimuli including tumor necrosis factor-α (TNFα), CD95 ligand, nerve growth factors and chemotherapeutic agents (Liu *et al.* 1997). The conversion of SM to ceramide has been suggested to regulate cell growth, differentiation, necrosis, proliferation, regeneration and apoptosis

(Bartke & Hannun 2009, Posse de Chaves 2006). Moreover, the generated ceramide tends to form ceramide-enriched domains which may facilitate and amplify the ceramide-related signalling pathway by clustering corresponding receptors such as CD95 (Zhang *et al.* 2009b). Thus, hydrolysis of SM can initiate the ceramide-associated signalling pathway. In addition, the synthesis of SM can also play a role in signalling transduction. In the plasma membrane, SMS2 utilizes phosphatidylcholine and ceramide as substrates to form SM and DAG. While this process may attenuate the ceramide-associated signalling pathway, the formation of DAG can in turn activate protein kinase C (PKC) (Goni & Alonso 1999).

3. SM-cholesterol interaction

SM consists of a phosphocholine headgroup, a sphingosine backbone and a long saturated amide-linked acyl chain (from 16 to 24 carbons) in most tissues, giving the SM molecule a fairly cylindrical molecular shape. The amide group at the 2 position and the hydroxyl group at the 3 position have the ability to both donate and accept hydrogen bonds (Fig. 1.3 A). Because of this property, SM has a natural tendency to form lipid rafts by attracting neighboring SM molecules (Ramstedt & Slotte 2002, Posse de Chaves & Sipione 2009). SM is well known for its tight interaction with cholesterol molecules in lipid rafts (Fig. 1.3 B), probably due to the hydrogen bonding of the 3-hydroxyl group of cholesterol to the amide group in SM, as well as the hydrophobic van der Waals interactions between the steroid ring of cholesterol and the saturated hydrocarbon chain of SM (Fig. 1.3 A) (Brown 1998, Ramstedt & Slotte 2002). In a recent report, charge-pairing between the positive charge of the nitrogen in the choline group on SM and the negative charge of the oxygen in the hydroxyl group on cholesterol was also indicated (Aittoniemi *et al.* 2007). SMase can destroy this tight interaction by catalyzing the hydrolysis of SM to ceramide and phosphocholine. Because of the disappearance of the interaction between the polar head of SM and the

neighbouring cholesterol, as well as the water-shield protection of SM's polar head for cholesterol, the affinity of ceramide for cholesterol is weaker (Fig. 1.3 C). Therefore, SM hydrolysis is expected to elevate the level of less organized cholesterol and ceramide, which may in turn affect the kinetics of the exocytosis. External application of C2, C6 or C18 ceramide has been shown to trigger the exocytosis in rat pheochromocytoma (PC12) cells (Tang et al. 2007). Ceramide has also been reported to activate selected isoforms of PKC (Fox *et al.* 2007, Huwiler *et al.* 1998). PKC is considered as a regulator for exocytosis. For example, the application of phorbol ester, the stimulator of PKC, has been suggested to enhance exocytosis from chromaffin cells (Knight & Baker 1983, Pocotte *et al.* 1985, Morgan & Burgoyne 1992) by increasing the size of the ready releasable pool of granules (Gillis *et al.* 1996). In spite of the increased number of exocytotic events, Q is decreased in phorbol ester-treated chromaffin cells, which is associated with faster release kinetics (Graham *et al.* 2000). The acceleration of fusion pore expansion resulting from the activation of PKC was also observed in horse eosinophils (Scepek *et al.* 1998). This change in release kinetics could be mimicked by the phosphomimetic mutation in PKC phosphorylation sites of Munc 18, which is an essential component helping with the formation of the SNAREs, indicating the phosphorylation of Munc 18 by PKC is responsible for the regulation of release kinetics (Barclay *et al.* 2003).

V. Role of cholesterol in quantal release

The cholesterol-rich lipid rafts in the plasma membrane have been reported to act as platforms for regulating exocytosis because of their ability to sequester specific proteins such as the SNAREs (Salaun *et al.* 2004). In presynaptic terminals, such lipid microdomains were also shown to contribute to the colocalization of VGCCs with the components of exocytotic machinery (Taverna *et al.* 2004). Studies on in PC12 cells suggest cholesterol extraction inhibited exocytosis (Lang *et al.* 2001a, Zhang *et al.* 2009a), although it is not

clear whether the inhibition was due to the disruption of the compartmentalization of the exocytotic process or the impairment of the calcium influx, because reduction in cholesterol has also been reported to inhibit VGCC function (Xia *et al.* 2008). In a recent study from our lab, whole-cell dialysis of a Ca^{2+}-buffered internal solution was employed as the trigger for exocytosis in rat chromaffin cells, thus bypassing any possible effect of changes in ion channels on exocytosis caused by cholesterol perturbation (Wang et al. 2010). Cholesterol, particularly that in the cytoplasmic leaflet of cellular membranes, was found to stabilize the fusion pore of LDCGs before the onset of rapid dilation (Wang et al. 2010).

VI. My hypothesis

In the plasma membrane, SM comprises 9.3% of total phospholipids and the SM to cholesterol molar ratio is up to 3:5 (Malviya *et al.* 1986). The goal of my thesis research was to determine the effects of SM hydrolysis on quantal release kinetics in chromaffin cells. Since cholesterol has been shown to retard the dilation of the semi-stable fusion pore (Wang et al. 2010) and SM hydrolysis by SMase can increase the levels of less organized cholesterol and ceramide, therefore, my working hypothesis is that SM hydrolysis can affect quantal release kinetics in rat chromaffin cells via elevation of free cholesterol and/or ceramide.

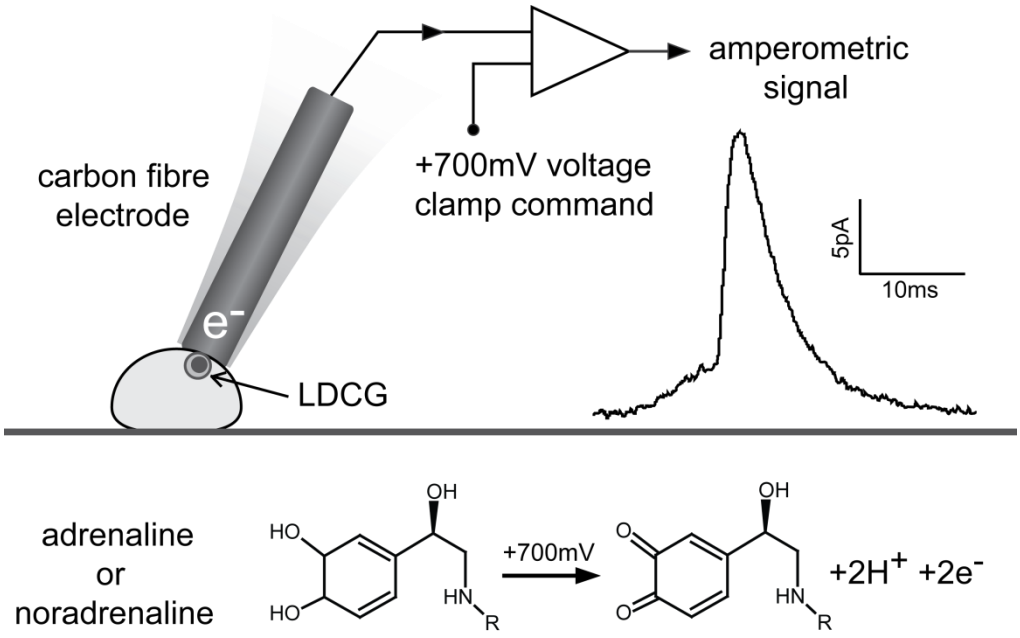

Figure 1.1 Scheme of amperometric recording from a chromaffin cell

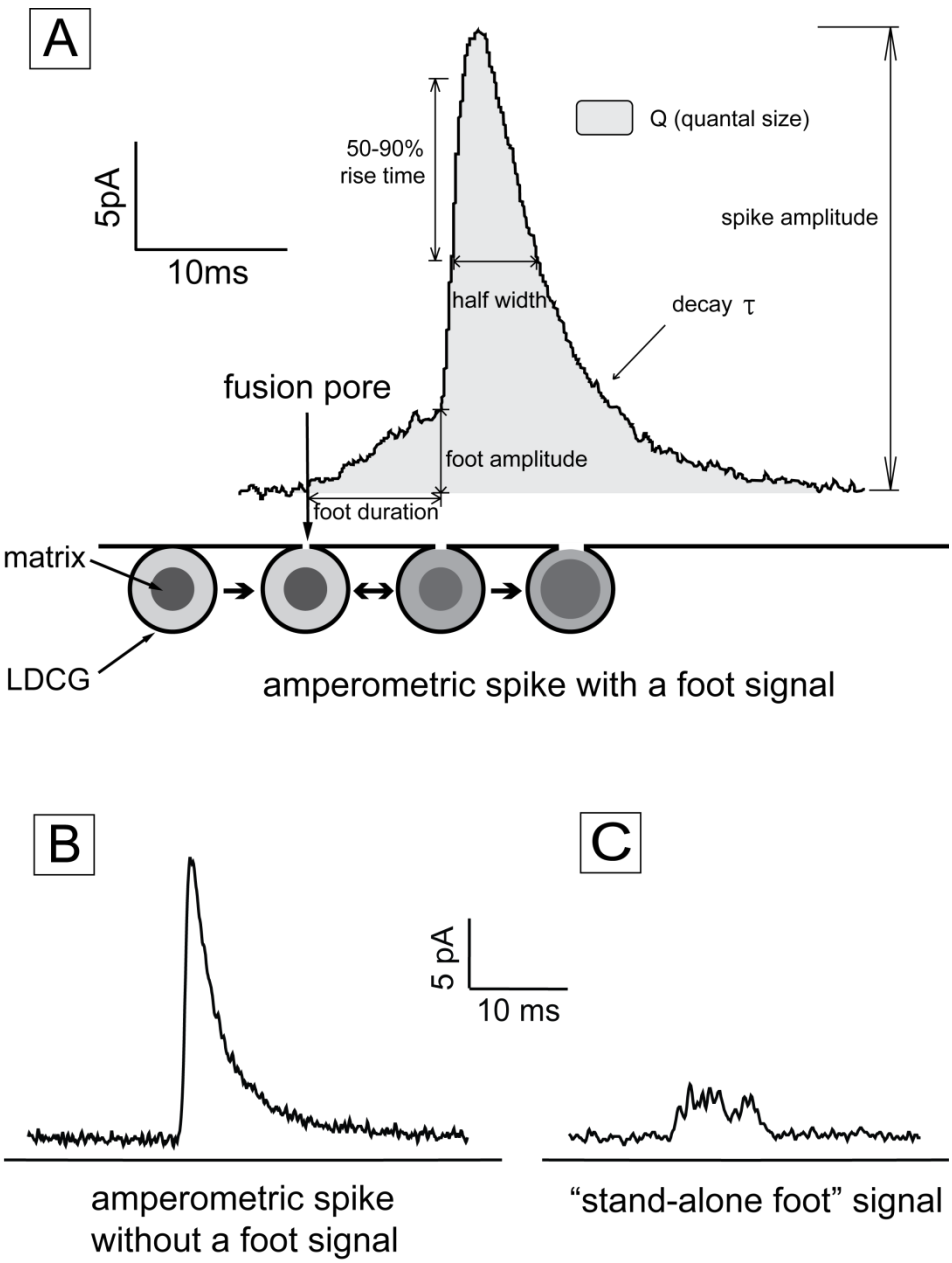

Figure 1.2 Examples of amperometric signals recorded from a rat adrenal chromaffin cell during the exocytosis of a LDCG. (A) amperometric signal with a foot signal; (B) amperometric signal without a foot signal; (C) "stand-alone foot" signal.

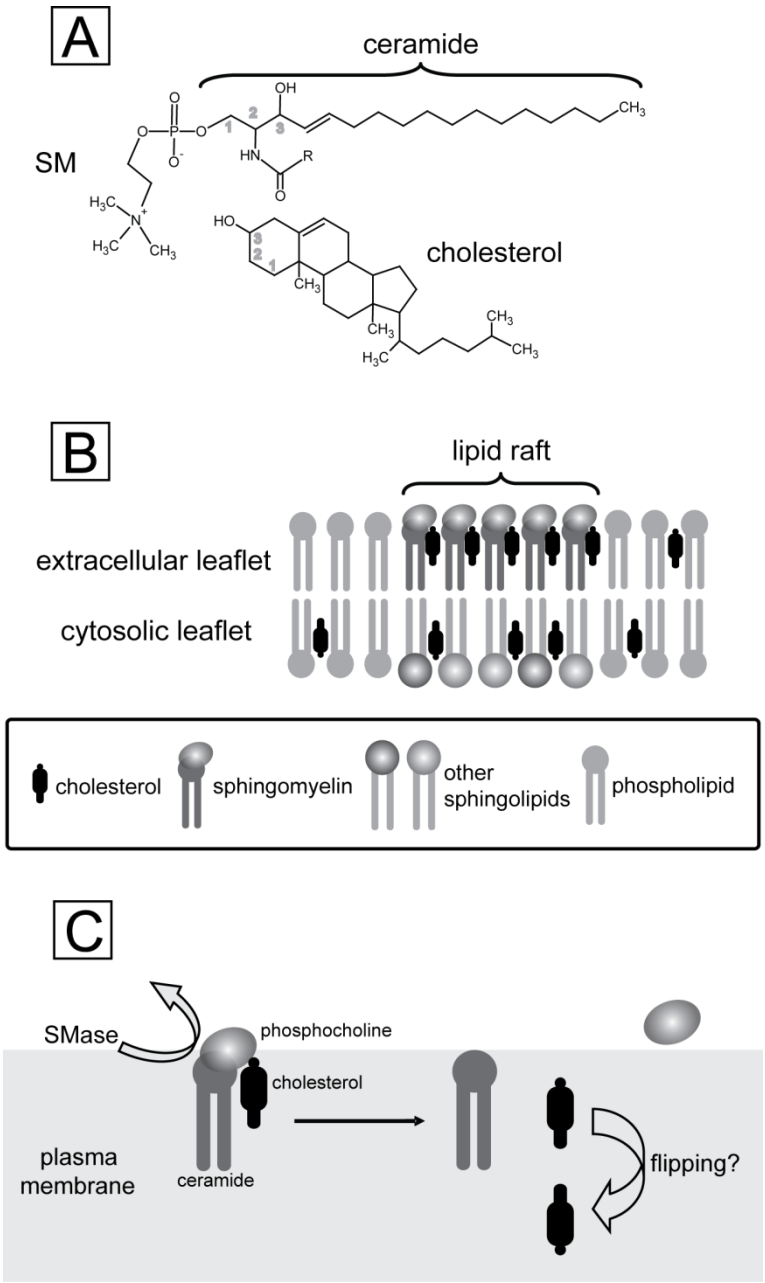

Figure 1.3 Interaction between sphingomyelin (SM) and cholesterol and liberation of cholesterol after hydrolysis of SM from a lipid raft**.** (A) SM consists of a phosphocholine headgroup, a sphingosine backbone and a long saturated amide-linked acyl chain represented as R. The amide group at the 2 position of SM may interact with the hydroxyl group at the 3 position of cholesterol. Charge-pairing between the positive charge of the nitrogen in the choline group on SM and the negative charge of the oxygen in the hydroxyl group on cholesterol was also indicated. In addition, hydrophobic van der Waals interactions exist between the steroid ring of cholesterol and the saturated hydrocarbon chains of SM; (B) SM can be concentrated in lipid rafts by a tight interaction with cholesterol; (C) Hydrolysis of SM by sphingomyelinase (SMase) can liberate cholesterol from lipid rafts.

References

Aittoniemi, J., Niemela, P. S., Hyvonen, M. T., Karttunen, M. and Vattulainen, I. (2007) Insight into the putative specific interactions between cholesterol, sphingomyelin, and palmitoyl-oleoyl phosphatidylcholine. *Biophys J,* **92,** 1125-1137.

Alberts, B., Bray, D., Lewis, J., Raff, M., Roberts, K. and Watson, J. D. (1994) *Molecular biology of the cell*. Garland Publishing, Inc, New York. 477-485.

Albillos, A., Dernick, G., Horstmann, H., Almers, W., Alvarez de Toledo, G. and Lindau, M. (1997) The exocytotic event in chromaffin cells revealed by patch amperometry. *Nature,* **389,** 509-512.

Barclay, J. W., Craig, T. J., Fisher, R. J., Ciufo, L. F., Evans, G. J., Morgan, A. and Burgoyne, R. D. (2003) Phosphorylation of Munc18 by protein kinase C regulates the kinetics of exocytosis. *J Biol Chem,* **278,** 10538-10545.

Barenholz, Y. and Thompson, T. E. (1980) Sphingomyelins in bilayers and biological membranes. *Biochim Biophys Acta,* **604,** 129-158.

Bartke, N. and Hannun, Y. A. (2009) Bioactive sphingolipids: metabolism and function. *J Lipid Res,* **50 Suppl,** S91-96.

Borges, R., Machado, J. D., Alonso, C., Brioso, M. A. and Gomez, J. F. (2000) Functional role of chromogranins. The intragranular matrix in the last phase of exocytosis. *Adv Exp Med Biol,* **482,** 69-81.

Brown, R. E. (1998) Sphingolipid organization in biomembranes: what physical studies of model membranes reveal. *J Cell Sci,* **111 (Pt 1),** 1-9.

Bruns, D., Riedel, D., Klingauf, J. and Jahn, R. (2000) Quantal release of serotonin. *Neuron,* **28,** 205-220.

Chow, R. H. and von Ruden, L. (1995) Single-Channel Recording. Plenum Press, New York.

Churchward, M. A., Rogasevskaia, T., Hofgen, J., Bau, J. and Coorssen, J. R. (2005) Cholesterol facilitates the native mechanism of Ca^{2+}-triggered membrane fusion. *J Cell Sci,* **118,** 4833-4848.

Davletov, B., Connell, E. and Darios, F. (2007) Regulation of SNARE fusion machinery by fatty acids. *Cell Mol Life Sci,* **64,** 1597-1608.

Edwards, A. V. and Jones, C. T. (1993) Autonomic control of adrenal function. *J Anat,* **183 (Pt 2),** 291-307.

Ferlinz, K., Linke, T., Bartelsen, O., Weiler, M. and Sandhoff, K. (1999) Stimulation of lysosomal sphingomyelin degradation by sphingolipid activator proteins. *Chem Phys Lipids,* **102,** 35-43.

Fox, G. Q. (1996) A morphometric analysis of exocytosis in KCl-stimulated bovine chromaffin cells. *Cell Tissue Res,* **284,** 303-316.

Fox, S. I. (2004) *Human physiology*. The McGrawn-Hill Companies, Inc., New York, NY 10020.

Fox, T. E., Houck, K. L., O'Neill, S. M. et al. (2007) Ceramide recruits and activates protein kinase C zeta (PKC zeta) within structured membrane microdomains. *J Biol Chem,* **282,** 12450-12457.

Futerman, A. H. and Riezman, H. (2005) The ins and outs of sphingolipid synthesis. *Trends Cell Biol,* **15,** 312-318.

Gillis, K. D., Mossner, R. and Neher, E. (1996) Protein kinase C enhances exocytosis from chromaffin cells by increasing the size of the readily releasable pool of secretory granules. *Neuron,* **16,** 1209-1220.

Gong, L. W., de Toledo, G. A. and Lindau, M. (2007) Exocytotic catecholamine release is not associated with cation flux through channels in the vesicle membrane but Na^+ influx through the fusion pore. *Nat Cell Biol,* **9,** 915-922.

Gong, L. W., Hafez, I., Alvarez de Toledo, G. and Lindau, M. (2003) Secretory vesicles membrane area is regulated in tandem with quantal size in chromaffin cells. *J Neurosci,* **23,** 7917-7921.

Goni, F. M. and Alonso, A. (1999) Structure and functional properties of diacylglycerols in membranes. *Prog Lipid Res,* **38,** 1-48.

Goni, F. M. and Alonso, A. (2002) Sphingomyelinases: enzymology and membrane activity. *FEBS Lett,* **531,** 38-46.

Graham, M. E., Fisher, R. J. and Burgoyne, R. D. (2000) Measurement of exocytosis by amperometry in adrenal chromaffin cells: effects of clostridial neurotoxins and activation of protein kinase C on fusion pore kinetics. *Biochimie,* **82,** 469-479.

Huitema, K., van den Dikkenberg, J., Brouwers, J. F. and Holthuis, J. C. (2004) Identification of a family of animal sphingomyelin synthases. *EMBO J,* **23,** 33-44.

Huwiler, A., Fabbro, D. and Pfeilschifter, J. (1998) Selective ceramide binding to protein kinase C-alpha and -delta isoenzymes in renal mesangial cells. *Biochemistry,* **37,** 14556-14562.

Knight, D. E. and Baker, P. F. (1983) The phorbol ester TPA increases the affinity of exocytosis for calcium in 'leaky' adrenal medullary cells. *FEBS Lett,* **160,** 98-100.

Kolodny, E. H. (2000) Niemann-Pick disease. *Curr Opin Hematol,* **7,** 48-52.

Koval, L. M., Yavorskaya, E. N. and Lukyanetz, E. A. (2001) Electron microscopic evidence for multiple types of secretory vesicles in bovine chromaffin cells. *Gen Comp Endocrinol,* **121,** 261-277.

Lang, T. (2007) SNARE proteins and 'membrane rafts'. *J Physiol,* **585,** 693-698.

Lang, T., Bruns, D., Wenzel, D., Riedel, D., Holroyd, P., Thiele, C. and Jahn, R. (2001a) SNAREs are concentrated in cholesterol-dependent clusters that define docking and fusion sites for exocytosis. *EMBO J,* **20,** 2202-2213.

Lang, T., Bruns, D., Wenzel, D., Riedel, D., Holroyd, P., Thiele, C. and Jahn, R. (2001b) SNAREs are concentrated in cholesterol-dependent clusters

that define docking and fusion sites for exocytosis. *Embo Journal,* **20,** 2202-2213.

Liu, B., Obeid, L. M. and Hannun, Y. A. (1997) Sphingomyelinases in cell regulation. *Semin Cell Dev Biol,* **8,** 311-322.

Liu, X., Zeidan, Y. H., Elojeimy, S. et al. (2006) Involvement of sphingolipids in apoptin-induced cell killing. *Mol Ther,* **14,** 627-636.

Lucic, D., Huang, Z. H., Gu, D., Subbaiah, P. V. and Mazzone, T. (2007) Cellular sphingolipids regulate macrophage apolipoprotein E secretion. *Biochemistry,* **46,** 11196-11204.

Malviya, A. N., Gabellec, M. M. and Rebel, G. (1986) Plasma membrane lipids of bovine adrenal chromaffin cells. *Lipids,* **21,** 417-419.

Morgan, A. and Burgoyne, R. D. (1992) Interaction between protein kinase C and Exo1 (14-3-3 protein) and its relevance to exocytosis in permeabilized adrenal chromaffin cells. *Biochem J,* **286 (Pt 3),** 807-811.

Mosharov, E. V. and Sulzer, D. (2005) Analysis of exocytotic events recorded by amperometry. *Nat Methods,* **2,** 651-658.

Plattner, H., Artalejo, A. R. and Neher, E. (1997) Ultrastructural organization of bovine chromaffin cell cortex-analysis by cryofixation and morphometry of aspects pertinent to exocytosis. *J Cell Biol,* **139,** 1709-1717.

Pocotte, S. L., Frye, R. A., Senter, R. A., TerBush, D. R., Lee, S. A. and Holz, R. W. (1985) Effects of phorbol ester on catecholamine secretion and protein phosphorylation in adrenal medullary cell cultures. *Proc Natl Acad Sci U S A,* **82,** 930-934.

Posse de Chaves, E. and Sipione, S. (2009) Sphingolipids and gangliosides of the nervous system in membrane function and dysfunction. *FEBS Lett*.

Posse de Chaves, E. I. (2006) Sphingolipids in apoptosis, survival and regeneration in the nervous system. *Biochim Biophys Acta,* **1758,** 1995-2015.

Rahamimoff, R. and Fernandez, J. M. (1997) Pre- and postfusion regulation of transmitter release. *Neuron,* **18,** 17-27.

Ramstedt, B. and Slotte, J. P. (2002) Membrane properties of sphingomyelins. *FEBS Lett,* **531,** 33-37.

Robinson, I. M., Finnegan, J. M., Monck, J. R., Wightman, R. M. and Fernandez, J. M. (1995) Colocalization of calcium entry and exocytotic release sites in adrenal chromaffin cells. *Proc Natl Acad Sci U S A,* **92,** 2474-2478.

Salaun, C., James, D. J. and Chamberlain, L. H. (2004) Lipid rafts and the regulation of exocytosis. *Traffic,* **5,** 255-264.

Scepek, S., Coorssen, J. R. and Lindau, M. (1998) Fusion pore expansion in horse eosinophils is modulated by Ca^{2+} and protein kinase C via distinct mechanisms. *EMBO J,* **17,** 4340-4345.

Schenck, M., Carpinteiro, A., Grassme, H., Lang, F. and Gulbins, E. (2007) Ceramide: physiological and pathophysiological aspects. *Arch Biochem Biophys,* **462,** 171-175.

Schuchman, E. H. (2007) The pathogenesis and treatment of acid sphingomyelinase-deficient Niemann-Pick disease. *J Inherit Metab Dis,* **30,** 654-663.

Simons, K. and Ikonen, E. (1997) Functional rafts in cell membranes. *Nature,* **387,** 569-572.

Tang, N., Ong, W. Y., Zhang, E. M., Chen, P. and Yeo, J. F. (2007) Differential effects of ceramide species on exocytosis in rat PC12 cells. *Exp Brain Res,* **183,** 241-247.

Taverna, E., Saba, E., Rowe, J., Francolini, M., Clementi, F. and Rosa, P. (2004) Role of lipid microdomains in P/Q-type calcium channel (Ca(v)2.1) clustering and function in presynaptic membranes. *Biol Chem,* **279,** 5127-5134.

Tuchmann, D. H., Auroux, M. and Haegel, P. (1972) *Illustrated human embryology,* Vol. 3. Masson and Company, 132-137.

Uchiyama, Y., Maxson, M. M., Sawada, T., Nakano, A. and Ewing, A. G. (2007) Phospholipid mediated plasticity in exocytosis observed in PC12 cells. *Brain Res,* **1151,** 46-54.

van Meer, G. and Holthuis, J. C. (2000) Sphingolipid transport in eukaryotic cells. *Biochim Biophys Acta,* **1486,** 145-170.

Verkleij, A. J., Zwaal, R. F., Roelofsen, B., Comfurius, P., Kastelijn, D. and van Deenen, L. L. (1973) The asymmetric distribution of phospholipids in the human red cell membrane. A combined study using phospholipases and freeze-etch electron microscopy. *Biochim Biophys Acta,* **323,** 178-193.

Vitale, N., Caumont, A. S., Chasserot-Golaz, S., Du, G., Wu, S., Sciorra, V. A., Morris, A. J., Frohman, M. A. and Bader, M. F. (2001) Phospholipase D1: a key factor for the exocytotic machinery in neuroendocrine cells. *EMBO J,* **20,** 2424-2434.

Wang, N., Kwan, C., Gong, X., de Chaves, E. P., Tse, A. and Tse, F. W. (2010) Influence of cholesterol on catecholamine release from the fusion pore of large dense core chromaffin granules. *J Neurosci,* **30,** 3904-3911.

Wasser, C. R., Ertunc, M., Liu, X. and Kavalali, E. T. (2007) Cholesterol-dependent balance between evoked and spontaneous synaptic vesicle recycling. *J Physiol,* **579,** 413-429.

Wightman, R. M., Troyer, K. P., Mundorf, M. L. and Catahan, R. (2002) The association of vesicular contents and its effects on release. *Ann N Y Acad Sci,* **971,** 620-626.

Xia, F., Xie, L., Mihic, A., Gao, X., Chen, Y., Gaisano, H. Y. and Tsushima, R. G. (2008) Inhibition of cholesterol biosynthesis impairs insulin secretion and voltage-gated calcium channel function in pancreatic beta-cells. *Endocrinology,* **149,** 5136-5145.

Zamir, O. and Charlton, M. P. (2006) Cholesterol and synaptic transmitter release at crayfish neuromuscular junctions. *J Physiol*, **571,** 83-99.

Zhang, J., Xue, R., Ong, W. Y. and Chen, P. (2009a) Roles of cholesterol in vesicle fusion and motion. *Biophys J*, **97,** 1371-1380.

Zhang, Y., Li, X., Becker, K. A. and Gulbins, E. (2009b) Ceramide-enriched membrane domains--structure and function. *Biochim Biophys Acta*, **1788,** 178-183.

Zhou, Z. and Misler, S. (1995a) Action potential-induced quantal secretion of catecholamines from rat adrenal chromaffin cells. *J Biol Chem*, **270,** 3498-3505.

Zhou, Z. and Misler, S. (1995b) Amperometric detection of stimulus-induced quantal release of catecholamines from cultured superior cervical ganglion neurons. *Proc Natl Acad Sci U S A*, **92,** 6938-6942.

Chapter 2: Materials and Methods

I. Chemicals and solutions

Unless specified otherwise, all chemicals were purchased from Sigma Chemical Co. (Oakville, ON, Canada). SMase from *Bacillus cereus* (previously described as nSMase) was kept as a stock solution (100 U/ml) in purified H_2O and stored at -20℃. Lovastatin was kept as stock solution (25mM) in ethanol and stored at 4 ℃ in the dark. C6 ceramide was purchased from Avanti Polar Lipids, Inc., (Alabaster, AL, U.S.A.) and kept as stock solution (10mM) in dimethyl sulfoxide (DMSO) and stored at -20℃. For all chemicals that were added to the culture medium, the stock solution was freshly diluted with the culture medium just before addition. The final concentrations of the different chemicals were as follows: SMase: 0.1 or 1U/ml; lovastatin: 5μM; methyl-β-cyclodextrin (MβCD): 5mM; C6 ceramide: 5μM; DMSO: 0.1%. Water-soluble cholesterol was first dissolved in purified H_2O at 2mg/ml, and then diluted to 0.1mg/ml with tissue culture medium. The standard bath solution contained (in mM): 150 NaCl, 2.5 KCl, 2 $CaCl_2$, 1 $MgCl_2$, 8 glucose, and 10 Na-Hepes (pH 7.4). To stimulate chromaffin cells, $[K^+]$ in the standard solution was raised to 50mM (equal molar replacement of NaCl by KCl). The phosphate-buffered saline (PBS, with 13mM phosphate) for the lipid assays contained (in g/l): 8 NaCl, 0.25 KCl, 0.24 KH_2PO_4 and 1.44 Na H_2PO_4 (pH 7.2).

II. Cell Preparation

Single rat chromaffin cells were prepared as described previously (Tang *et al.* 2007a). Briefly, male Sprague-Dawley rats (200-250g) were sacrificed in accordance with the standards of the Canadian Council on Animal Care. The adrenal medulla were dissociated enzymatically in a modified Hank's solution containing collagenase type I (3.0mg/ml), hyaluronidase type I-S (2.4mg/ml) and deoxyribonuclease type I (0.2mg/ml)

for 30min, followed by incubation with trypsin type I (0.5mg/ml) for 5min at 37℃. For amperometry experiments, single chromaffin cells were plated on uncoated plastic culture dishes (Corning 430166, Fisher Scientific Ltd., Ottawa, ON, Canada). For $[Ca^{2+}]_i$ measurements, single chromaffin cells were plated on uncoated glass coverslips that were cleaned with ~70% nitric acid. Cells were maintained in a defined medium (MEM) supplemented with 1% (v/v) insulin-transferrin-selenium-A (ITS), 50U/ml penicillin G and 50μg/ml streptomycin (Gibco, Grand Island, NY, U.S.A.). Recordings were performed at room temperature (20-24 ℃) on cells maintained in culture for 12-24hrs.

III. Determination of cellular SM content

Dissociated chromaffin cells were grown in a 24-well plate (Corning Inc., Corning, NY, U.S.A.). Cells were treated with 1U SMase for 1hr or 0.1U SMase overnight (15-20hrs). Untreated cells with the same duration of culture and mock solution changes were used as control. The harvesting and lysing of cells were performed on ice: the medium was removed from each well and cells were rinsed extensively with PBS. Cells were harvested and lysed by scraping with a plastic pipette tip in 175μl of radioimmunoprecipitation assay buffer (RIPA buffer; Pierce, Thermo Fisher Scientific Inc., Rockford, MD, U.S.A.). To determine protein content, 25μl of the cell lysate was used in a bicinchoninic acid protein assay kit (BCA protein assay kit) (Pierce). The remaining 150μl of cell lysate was diluted to 1ml (with purified H_2O) for the SM assay.

To minimize the interference from proteins and other water-soluble substances with the SM assay, lipid extraction was performed before the SM assay. The extraction procedure was modified from Bligh and Dyer (1959). Briefly, 1ml of cell lysate was vortexed with 3ml of chloroform/methanol (2:1 v/v) for 1min. The mixture was then centrifuged at 2000rpm for 10min. Following the removal of the supernatant, the extracted lipids at the bottom of the glass tube were washed with 2 ml of methanol/water (1:1 v/v) and then

dried under a gentle stream of nitrogen. The extracted lipids were then quantified by the SM assay kit (Cayman Chemical Company, Ann Arbor, MI, U.S.A.). To minimize the variation between experiments, the SM content in each treatment was first normalized to the protein content and then normalized to the corresponding control.

The protein assay (BCA protein assay kit) is based on the ability of proteins to reduce Cu^{2+} to Cu^{+} in an alkaline medium. Each Cu^{+} is then chelated by 2 molecules of bicinchoninic acid, giving rise to a purple-colored product with a strong absorbance at 562 nm (Smith *et al.* 1985, Wiechelman *et al.* 1988). The increase in absorbance is measured with a SpectraMax 190 plate reader (λ_{abs} 562 nm) whose linearity is confirmed by serial dilution of the protein standards in the kit. In the SM assay (with SM assay kit), SM is first hydrolyzed to phosphocholine and ceramide by SMase. The phosphocholine is then catalyzed by alkaline phosphatase to yield choline, which subsequently generates H_2O_2 in a reaction oxidized by choline oxidase. Finally, catalyzed by peroxidise, the newly formed H_2O_2 reacts with the N-ethyl-N-(2-hydroxy-3-sulfopropyl)-3,5-dimethoxyaniline, sodium salt (DAOS) and 4-aminoantipyrine to produce a blue product with an optimal light absorbance at 595 nm (Hojjati & Jiang 2006). The increase in absorbance is monitored in a SpectraMax 190 plate reader (λ_{abs} 595 nm).

IV. Determination of cellular cholesterol content

Cellular cholesterol content was examined in two experiments with different treatments. In the first experiment, there were 3 groups of cells: control, 1U SMase for 1hr and 0.1U SMase overnight. In the second experiment, some cells were treated with methyl-β-cyclodextrin (MβCD; 5mM) for 1hr to extract cellular cholesterol. In this experiment, there were four groups of cells: control, MβCD, 1U SMase for 1hr+MβCD and 0.1U SMase overnight+MβCD. Cells were harvested and lysed by scraping with a plastic pipette tip in 100μl RIPA buffer (Pierce). For protein assay, 50μl of the cell

lysate was used with the BCA protein assay kit (Pierce), and the remaining 50μl was used for the cholesterol assay with an Amplex Red cholesterol assay kit (Invitrogen, Burlington, ON, Canada).

In the cholesterol assay, cholesterol esters are first hydrolyzed into cholesterol by cholesterol esterase, and then all free cholesterol is oxidized by cholesterol oxidase to generate H_2O_2 and the corresponding ketone product. In the presence of horseradish peroxidise, H_2O_2 reacts with 10-acetyl-3,7-dihydroxyphenoxazine (Amplex Red reagent) to produce the highly fluorescent resorufin (Zhou *et al.* 1997). The increase in fluorescence is monitored in a SpectraMax Gemini XPS plate reader (λ_{ex} 545 nm; λ_{em} 590 nm) whose linearity is confirmed by serial dilution of the cholesterol standards in the kit.

V. Measurement of $[Ca^{2+}]_i$

$[Ca^{2+}]_i$ was monitored with digital imaging using a Tillvision imaging system equipped with Polychrome II high speed monochromator (Applied Scientific Instrument, Eugene, OR, USA) as described previously (Xu *et al.* 2003). Cells were loaded with fura-2 AM (2.5μM) in standard bath solution at 37℃ for 20min and then washed with standard bath solution for 10 min before recording. $[Ca^{2+}]_i$ was calculated from the ratio (R) of fluorescence (340/380 nm for fura-2), using the following equation (Grynkiewicz *et al.* 1985): $[Ca^{2+}]_i = K^*(R–R_{min})/(R_{max}–R)$, where R_{min} is the fluorescence ratio of Ca^{2+}-free indicator and R_{max} is the ratio of Ca^{2+}-bound indicator. K^* is a constant that was previously determined with the following procedure: single cells were dialyzed (via the whole-cell pipette) with three whole-cell pipette solutions with different known $[Ca^{2+}]$ as described previously (Tse *et al.* 1995). For all fura-2 measurements shown here, the values for R_{min}, R_{max} and K* were 0.13, 3.4 and 2.72mM, respectively (calibrated by Dr. Andy Lee).

VI. Electrical detection of catecholamine release

Carbon fibre (tip diameter of 7μm) amperometry (Wightman *et al.* 1991) was employed to monitor quantal catecholamine release at ms resolution from single rat chromaffin cells as previously described (Tang et al. 2007a). The fabrication of carbon fibre electrodes was as described by Zhou and Misler (1995a). Briefly, the carbon fibre electrode was first insulated with polyethylene (melted with a heating coil to form a thinly insulated region of ~150μm in length). The tip was then cut to a final length of ~20μm because the electrode noise largely depends on the electrode capacitance, which is proportional to the length of the insulated tip. During recording, the tip of the carbon fibre electrode was gently positioned to touch the cell surface. A +700mV potential (D.C.) was applied to the carbon fibre electrode using a VA-10 amplifier (NPI Electronics, Tamm, Germany). Chromaffin cells were initially bathed in the standard bath solution. To trigger catecholamine release, individual chromaffin cells were stimulated by bath application of a high $[K^+]$ (50mM) extracellular solution, which typically raised intracellular $[Ca^{2+}]_i$ to 0.5–1μM for minutes (Xu & Tse 1999). In all amperometry experiments, data were collected for 5min after the first event was detected. The sensitivity of 7 carbon fibre electrodes was examined by the application of 50μM noradrenaline (Camacho *et al.* 2006). The oxidation current was 118.8±12.2pA with a maximal variation of less than 27% among electrodes. To further minimize the slight variation in the sensitivity of individual carbon fibre electrodes, each electrode was used for one control cell and 2 or 3 cells in the treatment group (in random order).

Amperometric currents were filtered at 1kHz using 8-pole low-pass Bessel filter (Frequency Devices 9L8L, Haverhill, MA, USA), sampled at 10kHz with the Fetchex function of pCLAMP version 6.03 (Axon Instruments) and then analyzed with the Mini Analysis Program version 5.24 (Synaptosoft Inc., Decatar, GA, USA). I restricted my analysis to individual non-overlapping amperometric signals using the following criteria as

described in our previous study (Tang *et al.* 2005): (i) the amplitude of the amperometric event must be > 5×rms noise; (ii) the time integral of the amperometric event must be > 5fC; (iii) the 50–90% rise-time must be < 5ms; (iv) the decay time constant must be < 40ms; and (v) the interval between the peaks of two adjacent amperometric events must be > 3× the decay time constant of the first amperometric event. To better compare the average kinetic parameters between different cells, only cells with more than 30 events were included in my analysis.

VII. Data analysis

All plots and statistical analysis were performed with Origin version 6.0 (Origin Lab Corporation, Northampton, MA, USA). Two methods were used to analyze the kinetic parameters of the amperometric signals. In the first method, the mean of mean cellular values was employed for comparison between different treatment groups in order to minimize the bias introduced by any overrepresentation of individual cells that contributed an exceptionally large number of signals. This was accomplished by calculating the mean for a specific kinetic parameter from all the events in one cell and then averaging the values from all the cells in the same treatment group (Colliver *et al.* 2000). In the second method, all the events in each treatment were grouped according to their quantal size, and the specific kinetic parameters were plotted as a function of $Q^{1/3}$. The second method was employed because a previous study in our lab (Tang et al. 2007a) showed that all kinetic parameters varied with $Q^{1/3}$, and some manipulations in my study may alter this relationship. In the experiments on electrical detection of catecholamine release and measurement of $[Ca^{2+}]_i$, a Student's *t*-test (two-population) was used when comparing mean cellular parameters between different treatment groups; in those of the lipid assay, a Student's *t*-test (one-population) was used when comparing mean normalized cellular SM or cholesterol content to control. All mean values are given as mean ± S.E.. Values with $p<0.05$ were considered statistically

significant. The symbol * denotes $p<0.05$, the symbol ** denotes $p<0.01$, and the symbol *** denotes $p<0.001$.

References

Bligh, E. G. and Dyer, W. J. (1959) A rapid method of total lipid extraction and purification. *Can J Biochem Physiol,* **37,** 911-917.

Camacho, M., Machado, J. D., Montesinos, M. S., Criado, M. and Borges, R. (2006) Intragranular pH rapidly modulates exocytosis in adrenal chromaffin cells. *J Neurochem,* **96,** 324-334.

Colliver, T. L., Hess, E. J., Pothos, E. N., Sulzer, D. and Ewing, A. G. (2000) Quantitative and statistical analysis of the shape of amperometric spikes recorded from two populations of cells. *J Neurochem,* **74,** 1086-1097.

Grynkiewicz, G., Poenie, M. and Tsien, R. Y. (1985) A new generation of Ca^{2+} indicators with greatly improved fluorescence properties. *J Biol Chem,* **260,** 3440-3450.

Hojjati, M. R. and Jiang, X. C. (2006) Rapid, specific, and sensitive measurements of plasma sphingomyelin and phosphatidylcholine. *J Lipid Res,* **47,** 673-676.

Smith, P. K., Krohn, R. I., Hermanson, G. T. et al. (1985) Measurement of protein using bicinchoninic acid. *Anal Biochem,* **150,** 76-85.

Tang, K. S., Tse, A. and Tse, F. W. (2005) Differential regulation of multiple populations of granules in rat adrenal chromaffin cells by culture duration and cyclic AMP. *J Neurochem,* **92,** 1126-1139.

Tang, K. S., Wang, N., Tse, A. and Tse, F. W. (2007) Influence of quantal size and cAMP on the kinetics of quantal catecholamine release from rat chromaffin cells. *Biophys J,* **92,** 2735-2746.

Tse, A., Tse, F. W. and Hille, B. (1995) Modulation of Ca^{2+} oscillation and apamin-sensitive, Ca^{2+}-activated K^{+} current in rat gonadotropes. *Pflugers Arch,* **430,** 645-652.

Wiechelman, K. J., Braun, R. D. and Fitzpatrick, J. D. (1988) Investigation of the bicinchoninic acid protein assay: identification of the groups responsible for color formation. *Anal Biochem,* **175,** 231-237.

Wightman, R. M., Jankowski, J. A., Kennedy, R. T., Kawagoe, K. T., Schroeder, T. J., Leszczyszyn, D. J., Near, J. A., Diliberto, E. J., Jr. and Viveros, O. H. (1991) Temporally resolved catecholamine spikes correspond to single vesicle release from individual chromaffin cells. *Proc Natl Acad Sci U S A,* **88,** 10754-10758.

Xu, J. and Tse, F. W. (1999) Brefeldin A increases the quantal size and alters the kinetics of catecholamine release from rat adrenal chromaffin cells. *J Biol Chem,* **274,** 19095-19102.

Xu, J., Tse, F. W. and Tse, A. (2003) ATP triggers intracellular Ca^{2+} release in type II cells of the rat carotid body. *J Physiol,* **549,** 739-747.

Zhou, M., Diwu, Z., Panchuk-Voloshina, N. and Haugland, R. P. (1997) A stable nonfluorescent derivative of resorufin for the fluorometric

determination of trace hydrogen peroxide: applications in detecting the activity of phagocyte NADPH oxidase and other oxidases. *Anal Biochem,* **253,** 162-168.

Zhou, Z. and Misler, S. (1995) Action potential-induced quantal secretion of catecholamines from rat adrenal chromaffin cells. *J Biol Chem,* **270,** 3498-3505.

Chapter 3: Results

I. Change in cellular SM content with SMase treatment

To determine whether the extracellular application of nSMase reduced the cellular SM content, I performed the SM assay and the BCA protein assay. Chromaffin cells were divided into 3 groups —control (untreated), cells treated with SMase (1U for 1hr) and cells treated with SMase (0.1U overnight). As shown in Fig. 3.1, treatment with SMase (1U for 1hr) caused a significant reduction (~20%) in the cellular SM content of chromaffin cells (p=0.003, Student's t-test (one-population)) when compared with control. For cells treated with SMase (0.1U overnight), a reduction trend (~14%) in cellular SM was not statistically significant from control values.

II. Effects of SMase on quantal release

When chromaffin cells were stimulated by elevating extracellular [K^+] for 5 minutes, amperometric signals could still be reliably recorded from individual cells treated with either 1U SMase for 1hr or 0.1U SMase overnight. However, the treatment with 1U SMase for 1hr tended to reduce the mean number of amperometric events (to ~83% that of control, p = 0.106, Student's t-test (two-population)), whereas the treatment with 0.1U SMase overnight caused a significant reduction (to ~70% events of control, p=0.003) (Fig. 3.2A). Both SMase treatments significantly increased the proportion of "stand-alone foot" signals. When the treatment was 1U SMase for 1hr, the proportion increased to roughly double that of controls (from 0.760±0.132% to 1.524±0.315%), while the treatment with 0.1U overnight increased this proportion to triple that of controls (from 0.760±0.132% to 2.346±0.485%) (Fig. 3.2B). As shown in Fig. 3.2C, there was no difference in the mean value (Fig. 3.2.1Ci) or the distribution of $Q^{1/3}$ (Fig. 3.2Cii) among the three treatment groups. SMase affected neither the mean proportion of events with a

foot signal (Fig. 3.2Di) nor the percentage of such signals in a range of different $Q^{1/3}$ (Fig. 3.2Dii).

I compared each kinetic parameter of the amperometric signals with two analyses: the first was the average of its mean cellular value; the second was its mean value at any narrow range of $Q^{1/3}$ (see Chapter 2 Section VII for details). With both analyses, neither SMase treatment caused any significant change in the spike amplitude (Fig. 3.3A), half width (Fig. 3.3B) or decay τ (Fig. 3.3C). In contrast, SMase clearly affected the foot signals. 1U SMase for 1hr caused a significant increase in foot duration (to ~1.4-fold of controls, from 6.565±0.154ms to 9.137±0.361ms), whereas 0.1U SMase overnight resulted in an even larger increase (to ~1.6-fold of controls, from 6.565±0.154ms to 10.325±0.464ms) (Fig. 3.4Ai). Similarly, for over a wide range of $Q^{1/3}$, both treatments clearly increased the foot duration, and the effect of 0.1U SMase overnight was larger than that of 1U SMase for 1hr (Fig. 3.4Aii). However, no change in foot amplitude for both treatments was observed for the mean cellular value (Fig. 3.4Bi) or at any particular range of $Q^{1/3}$ (Fig. 3.4Bii). The increase in foot duration without a change in the foot amplitude resulted in a significantly larger foot area (Fig. 3.4C). Moreover, because SMase did not change Q (Fig. 3.2C), the increase in foot area also resulted in a larger fractional release during the foot portion of individual amperometric signals (Fig. 3.4D).

In summary, SMase treatment reduced the number of evoked amperometric events, but increased the proportion of “stand-alone foot” signals, the foot duration, the foot area and the fractional release during the foot signal. Note that in all these aspects, the effects of 1U SMase for 1hr (which reduced cellular SM significantly) were less robust than those of the treatment with a 10-fold lower concentration but for a longer time (overight:15-20hrs, which caused a statistically insignificant reduction in cellular SM).

III. The effects of SMase on quantal release mimics those of cholesterol overload

The overall effects of SMase on quantal release with elevated extracellular [K^+] as the trigger for exocytosis are very similar to those of cholesterol overload while amperometric signals were triggered by whole-cell dialysis of an intracellular solution with [Ca^{2+}] elevated to ~0.5μM, except the latter caused no significant reduction in the number of amperometric signals (Wang et al. 2010). Therefore, I compared the effects of both treatments with the same trigger (elevated extracellular [K^+]) for exocytosis, to test whether the effects of SMase treatment can completely mimic those of cholesterol overload.

For this comparison, dissociated chromaffin cells were treated for 1hr immediately before amperometric experiments with either 1U SMase, or 0.1mg/ml cholesterol, or both simultaneously; and untreated cells were used as controls. Treatment with SMase (1U for 1hr) shows a trend to reduce the mean number of amperometric events over the duration of 5 min (to ~85% events of control); cholesterol overload also tended to decrease exocytotic events (to ~64% events of control); when both treatments were combined, the reduction was even more severe (to ~56% events of control, p=0.023) (Fig. 3.5A). In comparison to the controls, the proportion of "stand-alone foot" signals increased ~3-fold with SMase (from 0.498±0.117% to 1.524±0.315%), while with cholesterol overload the increase was ~6-fold (2.984±1.298%). Most interestingly, when both treatments were applied, the proportion of "stand-alone foot" signals increased to ~12-fold that of controls (5.847±1.479%) (Fig. 3.5B). However, there was no significant difference among all the treatments groups in Q (Fig. 3.5C) or the proportion of events with a foot signal (Fig. 3.5D). Also, none of the treatments caused a significant change in any kinetic parameter of the spike portion of the amperometric signals (i.e. their amplitude, half width or decay τ; Fig. 3.6).

In contrast, SMase significantly prolonged the foot duration by ~40% (from 6.468±0.195ms to 9.137±0.361ms) and cholesterol overload prolonged it by ~30% (8.412±0.922ms). Interestingly, the combination of both treatments increased the foot duration by ~74% (11.286±1.014ms), as if the two effects of the two treatments were roughly additive (Fig. 3.7Ai). The plot of the trend of the change in foot duration at different values of $Q^{1/3}$ (Fig. 3.7Aii) suggests that effects of each treatment affected the foot duration over essentially the entire range of $Q^{1/3}$. However, none of the treatment groups affected the foot amplitude significantly (Fig. 3.7B). And the changes in the foot duration largely account for the changes in foot area (Fig. 3.7C) and fractional release during foot (Fig. 3.7D).

In summary, while the number of amperometric signals tended to be reduced by either cholesterol overload or SMase, this effect became statistically significant only when both treatments were combined. Also, while either treatment increased the proportion of "stand-alone foot" signals and the duration of the foot signal that precedes the amperometric spike, these effects became larger when the two treatments were combined.

IV. The effects of SMase on quantal release can be reduced by cholesterol extraction.

1. The effect of SMase (1U for 1hr) can be eliminated by cholesterol extraction

The results in the previous sections were consistent with the hypothesis that SMase exerts its influence on exocytosis by elevating the free cholesterol in the plasma membrane. To further examine this hypothesis, I tested whether the effect of SM hydrolysis could be reduced by the addition of the cholesterol extractor, MβCD, during the SMase treatment.

In this series of experiments, chromaffin cells were treated (for 1hr immediately before amperometric recording) either with 1U SMase, or 5mM MβCD, or both 1U SMase and 5mM MβCD simultaneously; untreated cells

served as controls. Fig. 3.8A shows that none of the treatment groups caused a significant inhibition of exocytosis. While the treatment with MβCD alone had no significant effect on the proportion of "stand-alone foot" signals, the inclusion of MβCD during SMase treatment essentially eliminated SMase's effect on increasing the proportion of "stand-alone foot" signals (Fig. 3.8B). None of the treatments had any significant effect on the $Q^{1/3}$ (Fig. 3.8C), the proportion of events with a foot signal (Fig. 3.8D) or the kinetic parameters of the main spike (Fig. 3.9). Most importantly, while MβCD alone had no significant effect on the duration (Fig. 3.10A) or amplitude (Fig. 3.10B) of the foot signal, the inclusion of MβCD during the treatment with SMase essentially eliminated SMase's effect on increasing the foot duration (which was otherwise detectable over a large range of $Q^{1/3}$ and was reflected in the roughly proportional changes in foot area (Fig. 3.10C) and fractional release during foot (Fig. 3.10D)).

In summary, the inclusion of a cholesterol extractor during the treatment with SMase (1U for 1hr) can essentially eliminate all the effects of SMase on the proportion of "stand-alone foot" signals and foot duration.

2. The effects of SMase (0.1U overnight) can be partially reduced by cholesterol extraction and inhibition of cholesterol synthesis

Since SMase is not expected to be membrane permeant, the application of extracellular SMase in the experiments described above was expected to hydrolyse SM mainly on the extracellular leaflet of the plasma membrane. It was probable that this action of extracellular SMase led to the redistribution of at least some cholesterol molecules that previously interacted tightly with the SM molecules in the extracellular leaflet to other sites of the plasma membrane. Cholesterol molecules (particularly those in less ordered domains) can flip between the two sides of a lipid bilayer, and a previous study in our lab showed that acute extraction of cholesterol from the cytosolic side of individual chromaffin cells was more effective in influencing the

amperometric signal (Wang et al. 2010). Moreover, my data in Sections I and II showed that, although 0.1 U SMase overnight hydrolysed less cellular SM than 1U SMase for 1hr, the effects of the former on amperometric signals were actually more robust than those of the latter. It is possible that the longer duration of the former manipulation led to more effective redistribution of cholesterol molecules away from the extracellular leaflet of the plasma membrane to other sites that are more relevant to influencing the kinetics of amperometric signals. To address this possibility, I examined whether the effects of 0.1U SMase overnight were equally sensitive to cholesterol extraction by the addition of MβCD (5mM) in the culture medium for 1hr.

In comparison to the experiments in Section IV.1, the duration of the SMase treatment in the present experiments was 14- to 19-fold longer, and the treated cells had more time to compensate for any resultant redistribution of cholesterol (e.g. by increasing the supply of newly synthesized cholesterol to the extracellular leaflet of the plasma membrane). To reduce this complication in the cells that received the cholesterol extraction treatment, I also limited their ability to resupply newly synthesized cholesterol anywhere in the cells by including an inhibitor of cholesterol synthesis (lovastatin, an HMG-CoA inhibitor that impedes the rate limiting step of cholesterol synthesis) in the culture medium for the entire duration of the SMase treatment.

As shown in Fig. 3.11A, the significant decrease in the number of events and the increase in the proportion of “stand-alone foot” signals caused by SMase treatment were essentially eliminated by including lovastatin during the SMase treatment followed by 1hr exposure to MβCD. These two additional manipulations affected neither the mean value nor the distribution for $Q^{1/3}$ (Fig. 3.11C) and the proportion of events with a foot signal (Fig. 3.11D). These manipulations also had no significant effect on the kinetic parameters of the main spike (Fig. 3.12), but partially reversed the increase in foot duration caused by SMase (from 10.325±0.464ms to 7.702±0.363ms, which is still significantly longer than control 6.700±0.249ms) (Fig. 3.13Ai).

This partial reduction of foot duration was detectable over essentially the entire range of $Q^{1/3}$ (Fig. 3.13Aii). None of the treatment groups changed the foot amplitude significantly, although this parameter tended to be smallest with the SMase+MβCD+lovastatin treatment (Fig. 3.13B). Correspondingly, the inclusion of MβCD and loavstatin during the SMase treatment essentially eliminated the effects of SMase on foot area (Fig. 3.13C) and fractional release during foot (Fig. 3.13D).

In summary, cholesterol extraction and the inhibition of its synthesis eliminated most of the effects resulting from SMase (0.1U overnight), including the decrease in amperometric signals from individual cells, as well as the increased proportion of "stand-alone foot" signals, foot area and fractional release during foot; however it only partially reversed the effect of SMase on foot duration.

V. The effects of SMase on quantal release cannot be mimicked by exogenous C6 ceramide overload

SM hydrolysis is not only expected to elevate the level of less organized cholesterol, but will also generate ceramide (usually C16-24 ceramide). Both cholesterol and ceramide may have effects on quantal release. Although the data presented so far strongly support the scenario that the effects of SMase on quantal release can be attributed to the elevation of less organized cholesterol, the possible contribution from elevation of cellular ceramide cannot be ruled out. To address this issue, I performed experiments that involved overloading chromaffin cells with exogenous ceramide. Since the SM molecules concentrated in the plasma membrane typically have acyl chains with 16-24 carbons, the ceramide molecules generated from them after SM hydrolysis are expected to have acyl chains of the same length; therefore ideally the overload experiments should involve such ceramides. However, the poor solubility of long chain ceramides (acyl chain with > 6 carbons) makes the delivery of such molecules to cells particularly challenging (Goni &

Alonso 2009). I confirmed that C16 ceramide was insoluble even in 100% DMSO. However, C6 ceramide (which poorly mimics the biophysical properties of longer chain ceramides in membranes, but can mimic longer chain ceramides in activating certain signalling pathways (see Chapter 1 Section IV.3 for details)) can be dissolved in 0.1% DMSO.

In this series of experiments, dissociated chromaffin cells were treated with 5μM C6 ceramide (with 0.1% DMSO as carrier) for 1hr immediately before the amperometric recording. To examine whether some effects of C6 ceramide are due to DMSO, cells were treated for the same duration with 0.1% DMSO. Untreated cells were used as controls. C6 ceramide caused a significant reduction in the number of exocytotic events (to ~50% events of control) (Fig. 3.14A). Most importantly, opposite to the effect of SMase, C6 ceramide dramatically reduced the proportion of "stand-alone foot" signals to only ~7% that of controls (Fig. 3.14B). It also reduced the Q of LDCG for the mean cellular value (by ~11% for $Q^{1/3}$, p=0.008) (Fig. 3.14Ci), and this reduction was probably related to a detectable increase in the proportion of events with very small Q ($Q^{1/3} < 0.25$ $pC^{1/3}$) (Fig. 3.14Cii). Moreover the proportion of amperometric spikes with a foot signal was significantly reduced by ~12% (Fig. 3.14Di), although no conspicuous change was detected when this parameter was compared at matched values of $Q^{1/3}$ (Fig. 3. 14Dii).

Because every kinetic parameter of amperometric signals varied with Q (Tang et al. 2007a), the comparison of the mean of cellular mean values of each specific spike parameter is less meaningful when there was even a significant difference in mean of the mean cellular values of Q. Since C6 ceramide actually affected both the mean cellular value and the distribution of $Q^{1/3}$, it is more appropriate to compare the plots of individual kinetic parameters at matched values of $Q^{1/3}$. C6 ceramide did not change any kinetic parameters of the main spike (Fig. 3.15) at any range of $Q^{1/3}$. However, it caused a detectable reduction in foot duration (but not the foot amplitude) at different values of $Q^{1/3}$ (Fig. 3.16Aii, Fig. 3.16Bii), which probably

contributed to a barely detectable decrease in the foot area (Fig. 3.16Cii) and the fractional release during foot (Fig. 3.16D) at certain values of $Q^{1/3}$.

For all of the kinetic parameters studied, there was no significant difference between the cells exposed to 0.1% DMSO alone for 1 hr and untreated controls. Therefore none of the effects observed with C6 ceramide can be attributed to the 0.1% DMSO solvent.

In summary, due to their poor solubility, ceramide molecules with the dominant acyl chain length (C16- C24) could not be added exogenously to the chromaffin cells. Instead, I employed C6 ceramide in my experiment and found that C6 ceramide significantly reduced the number of amperometric signals, their mean Q value, as well as the proportion of "stand-alone foot". At matched values of $Q^{1/3}$, C6 ceramide caused a discernable decrease in foot duration. Most importantly, C6 ceramide and SMase had opposite effects on the two parameters, which may reflect the stability of an undilated fusion pore: the proportion of "stand-alone foot" signals and the foot duration.

VI. Change in detected cellular cholesterol content with SMase treatment

The data in Sections III to V showed that effects of SMase on quantal release mimicked those of cholesterol overload rather than C6 ceramide overload, and could be reduced by cholesterol extraction. Overall these findings are consistent with the possibility that the effects of SMase involved the redistribution of cholesterol molecules away from their tight interaction with SM to sites that influence the amperometric foot signals. Furthermore, Sections I and II showed that the treatment with 0.1U SMase overnight had larger effects on both types of amperometric signals than the treatment with 0.1U SMase for 1hr, although the two procedures caused similar reductions in cellular SM. It is possible that the longer duration of the former treatment allowed more cholesterol molecules that were previously interacting with SM to redistribute to other sites where they could regulate the amperometric foot signals. To further explore this issue I compared the cellular level of readily

detectable cholesterol under the experimental conditions that were described earlier. It turned out that the level of readily detectable cholesterol in cells was actually increased (by 14% or 15%, respectively) after the treatment with 1U SMase for 1hr or with 0.1U SMase overnight; the effect of the former treatment was even statistically significant ($p<0.001$, Student's *t*-test (one-population)), but the latter did not cause a significant effect (Fig. 3.17A). Moreover, the extraction of cellular cholesterol by MβCD (5mM for 1hr) tended to be less effective when MβCD was applied either simultaneously with 1U SMase (also for 1hr) or immediately after overnight 0.1U SMase treatment (Fig. 3.17B).

The overall results from this Section are consistent with the following scenario: SMase treatment redistributes some cellular cholesterol into certain more readily detectable pools that may also be more resistant to extraction by MβCD. However, these results provided no support for the possibility that the two SMase treatments redistributed cellular cholesterol to different extents.

VII. Change in the depolarization-evoked Ca^{2+} signal with SMase treatment and cholesterol overload

The data in Sections II and III showed that fewer amperometric events tended to be triggered from cells treated for 1hr with either 1U SMase or cholesterol, while the overnight treatment with 0.1U SMase caused a statistically significant decrease in the number of amperometric signals recorded from individual cells. Moreover, in all of these treatment groups both the proportion of stand alone foot signals and the duration of the prespike foot signal were significantly increased. The perturbation of cholesterol was reported to change the function of VGCC in different cell types (Xia et al. 2008, Xia *et al.* 2007), and this effect may have secondary influences on the triggering and kinetics of amperometric signals (Scepek et al. 1998, Fernandez-Chacon & Alvarez de Toledo 1995, Elhamdani *et al.* 2001).

To address this issue, I employed digital imaging of a ratiometric fluorescent [Ca^{2+}] indicator (fura-2 AM) to explore if my key experimental manipulations altered the peak increase in $[Ca^{2+}]_i$ ($\Delta[Ca^{2+}]_i$) that was triggered by exposing cells to elevated (50mM) extracellular [K^+]. Fig. 3.18 shows that compared to controls, SMase (1U for 1hr) or cholesterol overload did not cause any significant change in the $\Delta[Ca^{2+}]_i$, but SMase (0.1U overnight) caused a small but significant decrease in $\Delta[Ca^{2+}]_i$ (by ~12%).

In summary, the data from the last experiment cannot rule out the possibility that my manipulations to perturb SM and/or cholesterol altered the triggering and kinetics of amperometric signals indirectly via VGCC function and [Ca^{2+}].

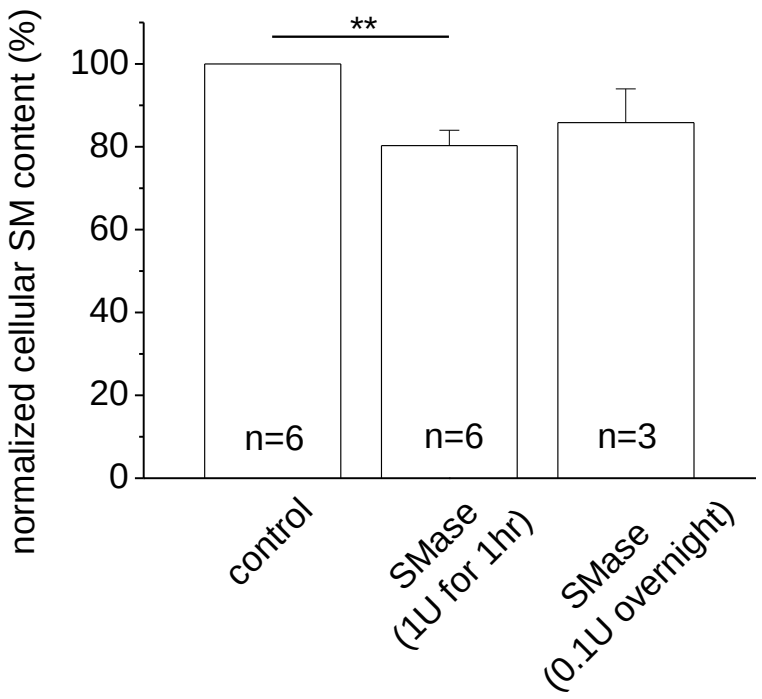

Figure 3.1 Effects of SMase on cellular SM content. Treatment with SMase (1U for 1hr) significantly reduced cellular SM content in rat chromaffin cells and treatment with SMase (0.1U overnight) tended to reduce it, but not statistically significant. The results of control and SMase (1U for 1hr) were obtained from 6 experiments, and that of SMase (0.1U overnight) was from 3 experiments. In each experiment, SM content was normalized to its corresponding control.

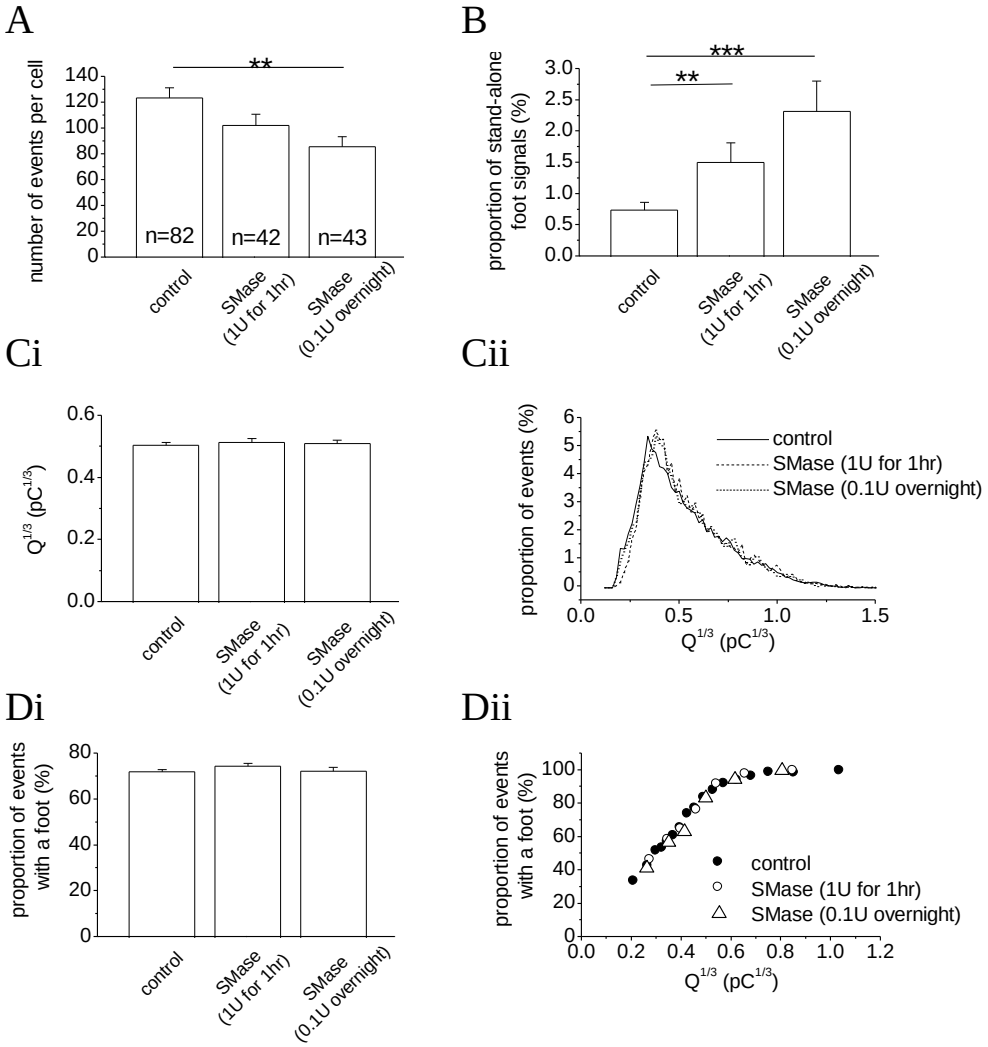

Figure 3.2 Effects of SMase (1U for 1hr or 0.1U overnight) on the number of events per cell, the proportion of "stand-alone foot" signals, the Q of the LDCGs (indicated by $Q^{1/3}$), and the proportion of events with a foot. (A) The number of events was reduced by both SMase treatments. Specifically, SMase (0.1U overnight) caused a significant reduction. (B) When compared to controls, the proportion of "stand-alone foot" signals was doubled or tripled in cells treated with SMase 1U for 1hr and 0.1U overnight respectively. (C) SMase did not change the mean value of $Q^{1/3}$ (Ci) or the frequency of events at different values of $Q^{1/3}$ (bin size of 0.02 $pC^{1/3}$; Cii). (D) SMase did not change the proportion of events with a foot (Di) or the frequency of events at different values of $Q^{1/3}$ (Dii). In (A-D), data were generated from 82 control cells (10,219 events), 42 cells (4,355 events) treated with SMase (1U for 1hr) and 43 cells (3,749 events) treated with SMase (0.1U overnight). Each data point in (Dii) was averaged from 600 events.

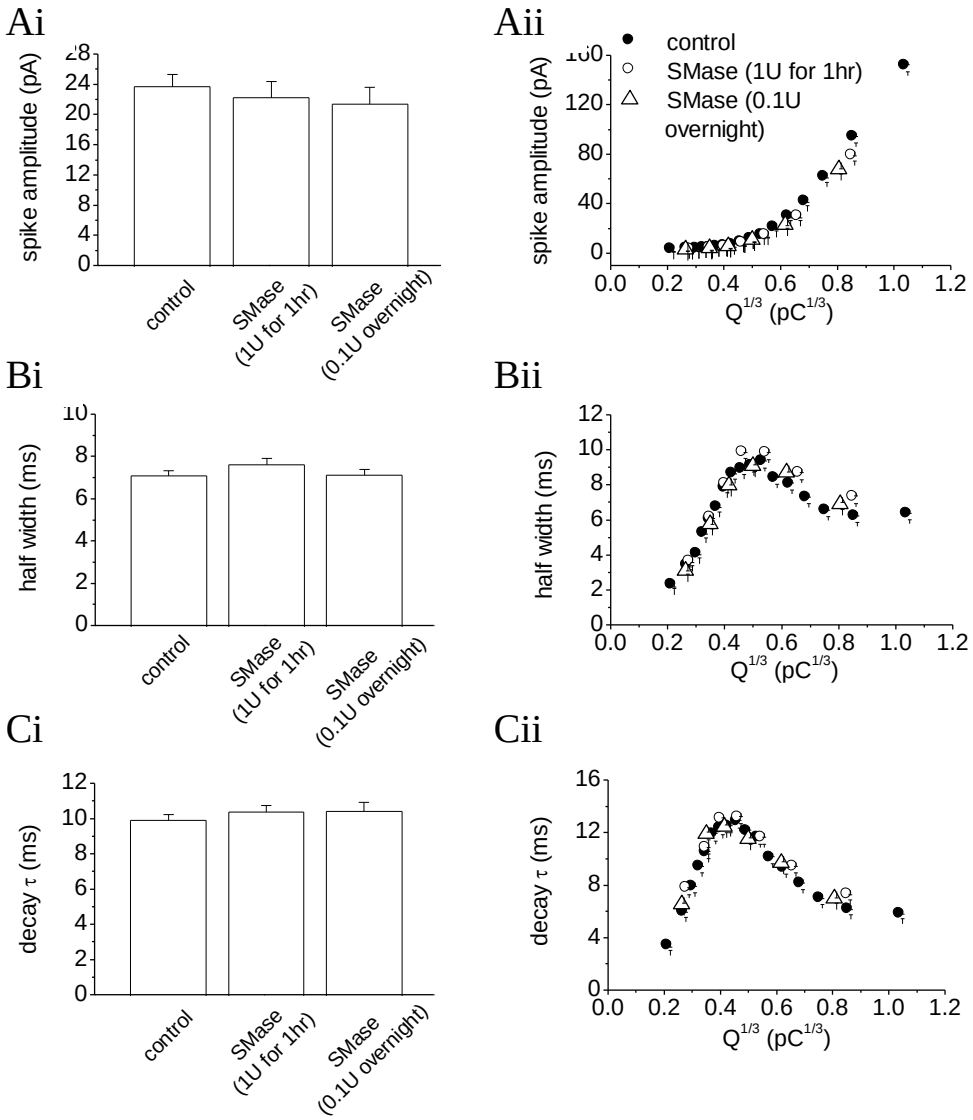

Figure 3.3 SMase did not affect the different kinetic parameters of the spike. Plots of the spike amplitude, half width, and decay τ for the mean cellular value (Ai, Bi and Ci) and at different values of $Q^{1/3}$(Aii, Bii and Cii) are shown. In (A-C), data were generated from 82 control cells (10,219 events), 42 cells (4,355 events) treated with SMase (1U for 1hr) and 43 cells (3,749 events) treated with SMase (0.1U overnight). Each data point in (Aii, Bii and Cii) was averaged from 600 events.

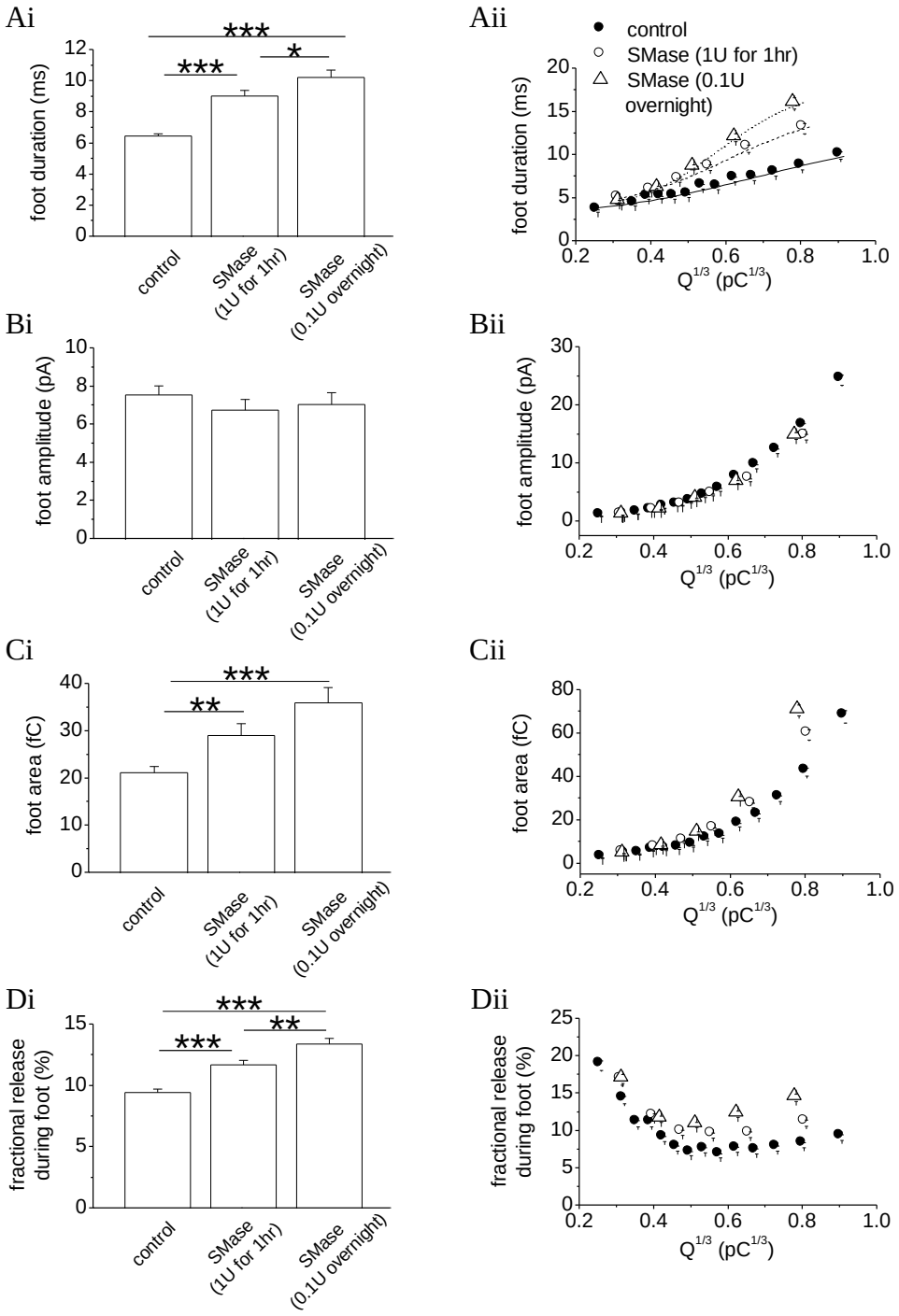

Figure 3.4 SMase increased the foot duration, the foot area and the fractional release during foot. (A) SMase (1U for 1hr) increased the foot duration to ~1.4-fold of controls and SMase (0.1U overnight) to ~1.6-fold of controls. (B) SMase had no significant effect on the foot amplitude. The changes in the foot duration resulted in the corresponding changes in the foot area (C) and the fractional release during foot (D). In (A-D), data were generated from 82 control cells (7,453 events), 42 cells (3,305 events) treated with SMase (1U for 1hr) and 43 cells (2,752 events) treated with SMase (0.1U overnight). Each data point in (Aii, Bii, Cii and Dii) was averaged from 500 events.

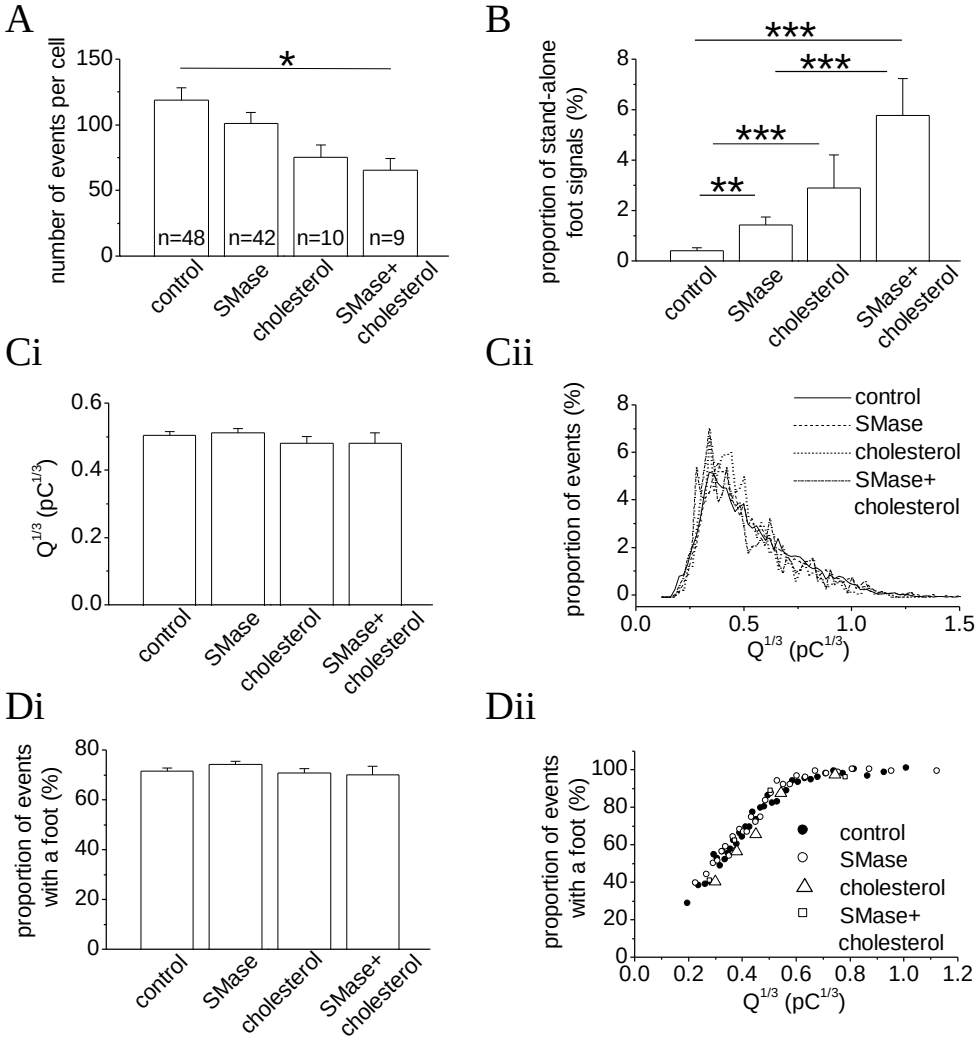

Figure 3.5 Effects of SMase (1U for 1hr), cholesterol (0.1mg/ml for 1hr) and 1hr treatment of SMase (1U)+cholesterol (0.1mg/ml) on the number of events per cell, the proportion of "stand-alone foot" signals, the Q of the LDCGs, and the proportion of events with a foot. (A) The number of events was reduced by SMase treatment and cholesterol overload, and SMase+cholesterol caused a significant reduction. (B) The proportion of "stand-alone foot" signals was increased to ~3-fold of controls by SMase, and to ~6-fold of controls by cholesterol overload. Most dramatically, SMase+cholesterol increased it to ~12-fold of controls. SMase, cholesterol and SMase+cholesterol did not change Q (C) or the proportion of events with a foot (D). In (A-D), data were generated from 48 control cells (5,774 events), 42 cells treated with SMase (4,355 events), 10 cells treated with cholesterol (770 events), and 9 cells treated with SMase+cholesterol (603 events). Each data point in (Dii) was averaged from 150 events.

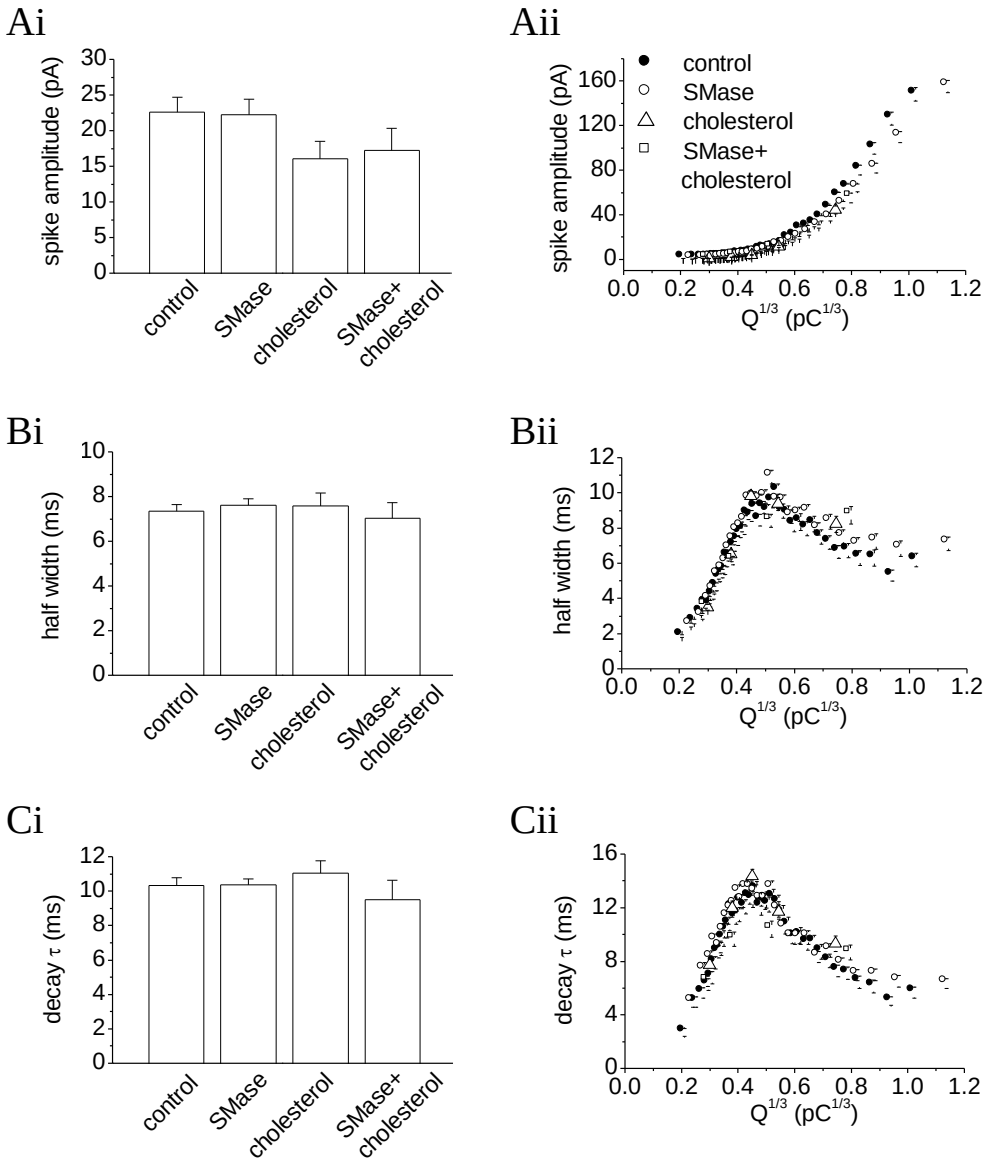

Figure 3.6 SMase (1U for 1hr), cholesterol (0.1mg/ml for 1hr) and 1hr treatment of SMase (1U)+cholesterol (0.1mg/ml) did not affect the different kinetic parameters of the spike. Plots of the spike amplitude, half width, and decay τ for the mean cellular value (Ai, Bi and Ci) and at different values of $Q^{1/3}$ (Aii, Bii and Cii) are shown. In (A-C), data were generated from 48 control cells (5,774 events), 42 cells treated with SMase (4,355 events), 10 cells treated with cholesterol (770 events), and 9 cells treated with SMase+cholesterol (603 events). Each data point in (Aii, Bii and Cii) was averaged from 150 events.

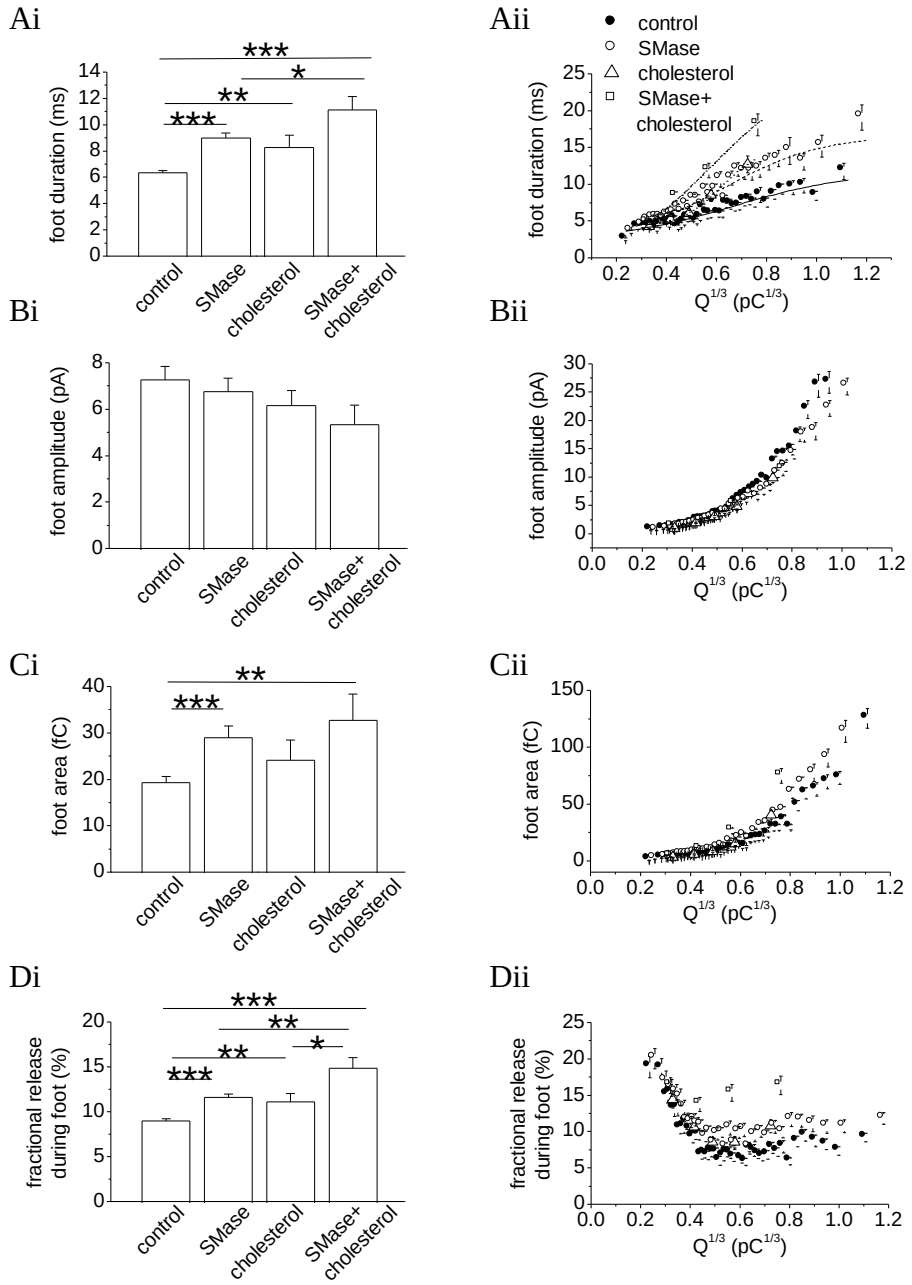

Figure 3.7 SMase (1U for 1hr), cholesterol (0.1mg/ml for 1hr) and 1hr treatment of SMase (1U)+cholesterol (0.1mg/ml) increased the foot duration, the foot area and the fractional release during foot. (A) The foot duration was increased to ~1.4-fold of controls by SMase, ~1.3-fold by cholesterol overload and ~1.7-fold by SMase+cholesterol. (B) SMase, cholesterol and SMase+cholesterol had no significant effects on the foot amplitude. The changes in the foot duration resulted in the corresponding changes in the foot area (C) and the fractional release during foot (D). In (A-D), data were generated from 48 control cells (4,227 events), 42 cells treated with SMase (3,305 events), 10 cells treated with cholesterol (549 events), and 9 cells treated with SMase+cholesterol (430 events). Each data point in (Aii, Bii, Cii and Dii) was averaged from 100 events.

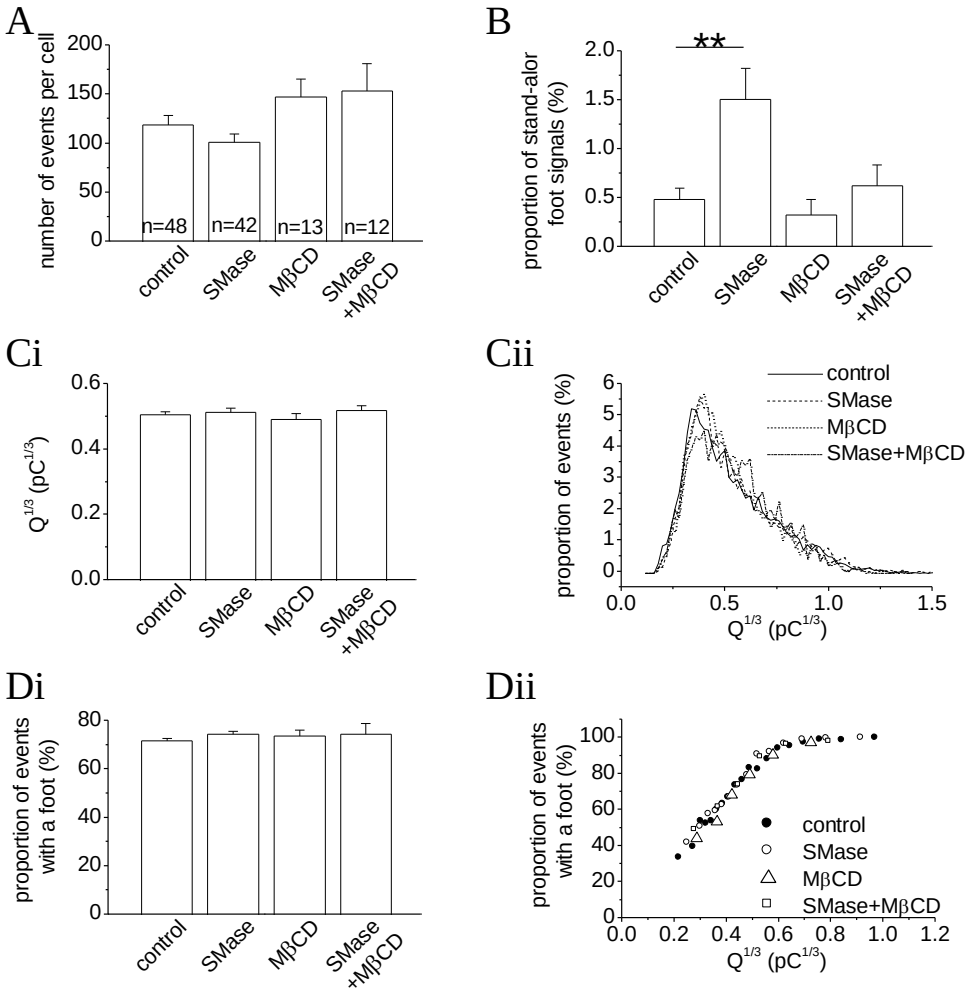

Figure 3.8 Effects of SMase (1U for 1hr), MβCD (5mM for 1hr) and 1hr treatment of SMase (1U)+MβCD (5mM) on the number of events per cell, the proportion of "stand-alone foot" signals, the Q of the LDCGs, and the proportion of events with a foot. (A) There was no significant difference in the number of events per cell in all treatment groups. (B) SMase increased the proportion of "stand-alone foot" signals to triple of controls, but this effect was eliminated by the application of MβCD, while MβCD alone did not affect it significantly. SMase, MβCD, and SMase+MβCD did not change Q (C) or the proportion of events with a foot (D). In (A-D), data were generated from 48 control cells (5,774 events), 42 cells treated with SMase (4,355 events), 13 cells treated with MβCD (1,934 events), and 12 cells treated with SMase+MβCD (1,861 events). Each data point in (Dii) was averaged from 300 events.

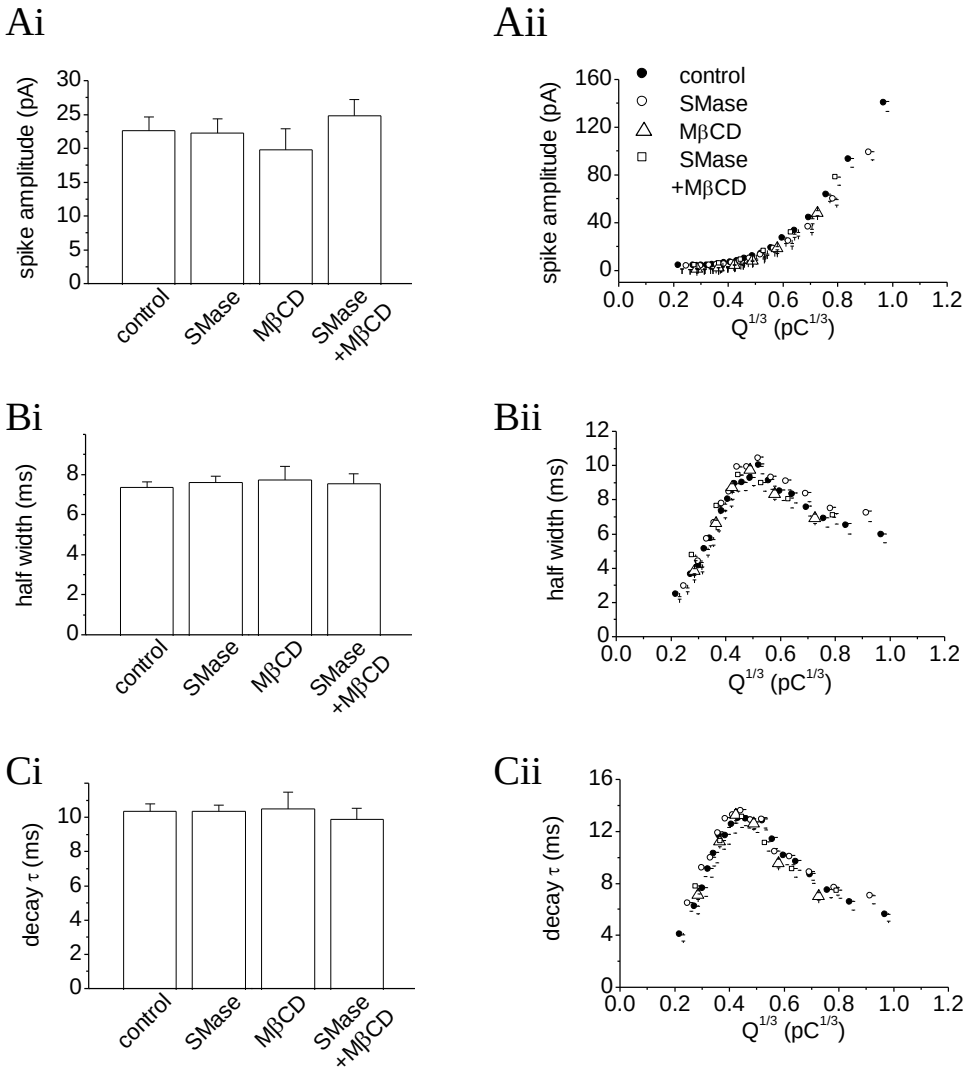

Figure 3.9 SMase (1U for 1hr), MβCD (5mM for 1hr) and 1hr treatment with SMase (1U)+MβCD (5mM) did not affect the different kinetic parameters of the spike. Plots of the spike amplitude, half width, and decay τ for the mean cellular value (Ai, Bi and Ci) and at different values of $Q^{1/3}$ (Aii, Bii and Cii) are shown. In (A-C), data were generated from 48 control cells (5,774 events), 42 cells treated with SMase (4,355 events), 13 cells treated with MβCD (1,934 events), and 12 cells treated with SMase+MβCD (1,861 events). Each data point in (Dii) was averaged from 300 events.

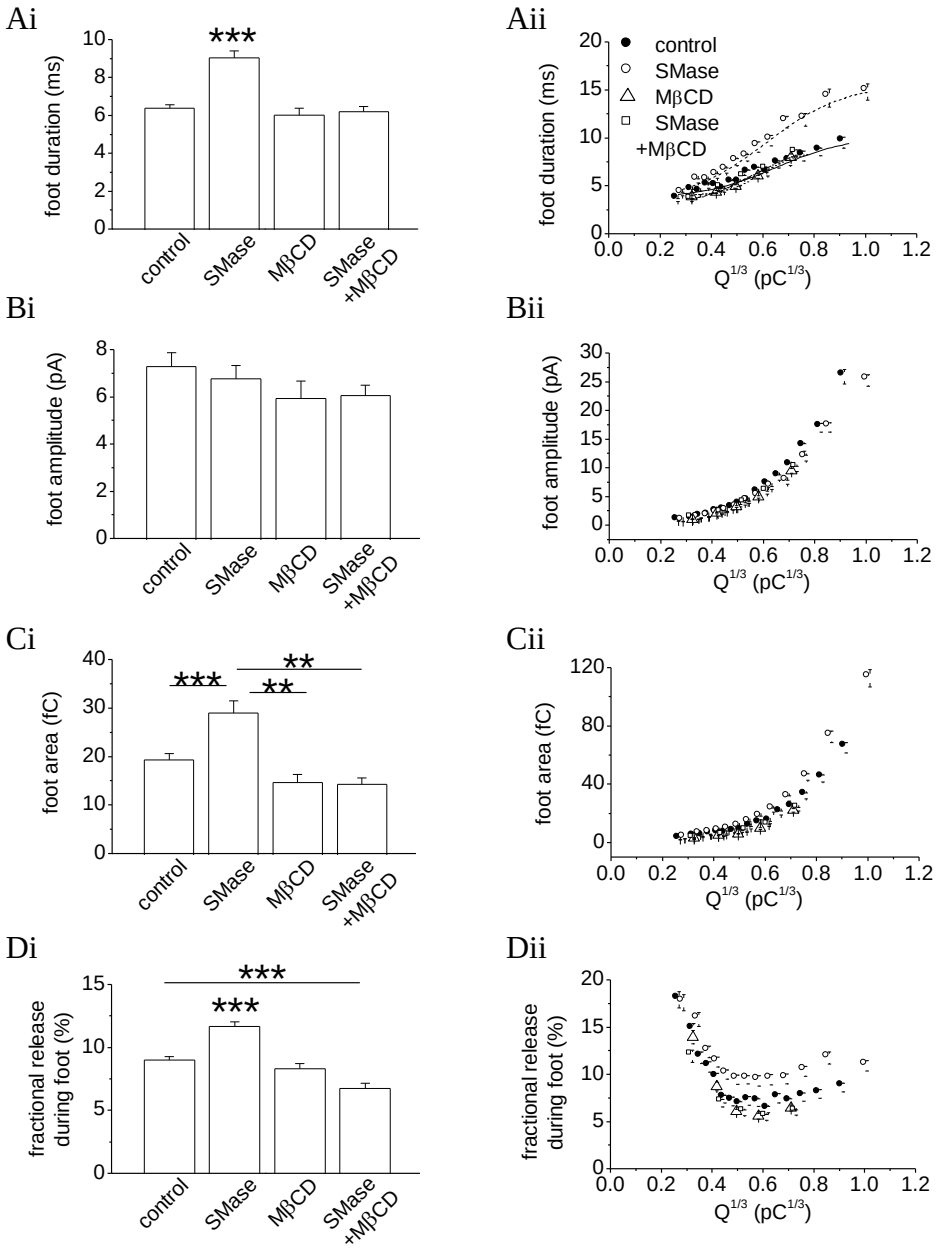

Figure 3.10 Effects of SMase (1U for 1hr), MβCD (5mM for 1hr) and 1hr treatment of SMase (1U)+MβCD (5mM) on the foot duration, the foot area and the fractional release during foot. (A) The increase in foot duration by SMase was eliminated by the application of MβCD, while MβCD alone did not affect it significantly. (B) SMase, MβCD, and SMase+MβCD had no significant effect on the foot amplitude. The changes in the foot duration resulted in the corresponding changes in the foot area (C) and the fractional release during foot (D). For SMase+MβCD treatment, the fractional release during foot is significantly smaller than controls (D). In (A-D), data were generated from 48 control cells (4,227 events), 42 cells treated with SMase (3,305 events), 13 cells treated with MβCD (1,934 events), and 12 cells treated with SMase+MβCD (1,861 events). Each data point in (Aii, Bii, Cii and Dii) was averaged from 250 events.

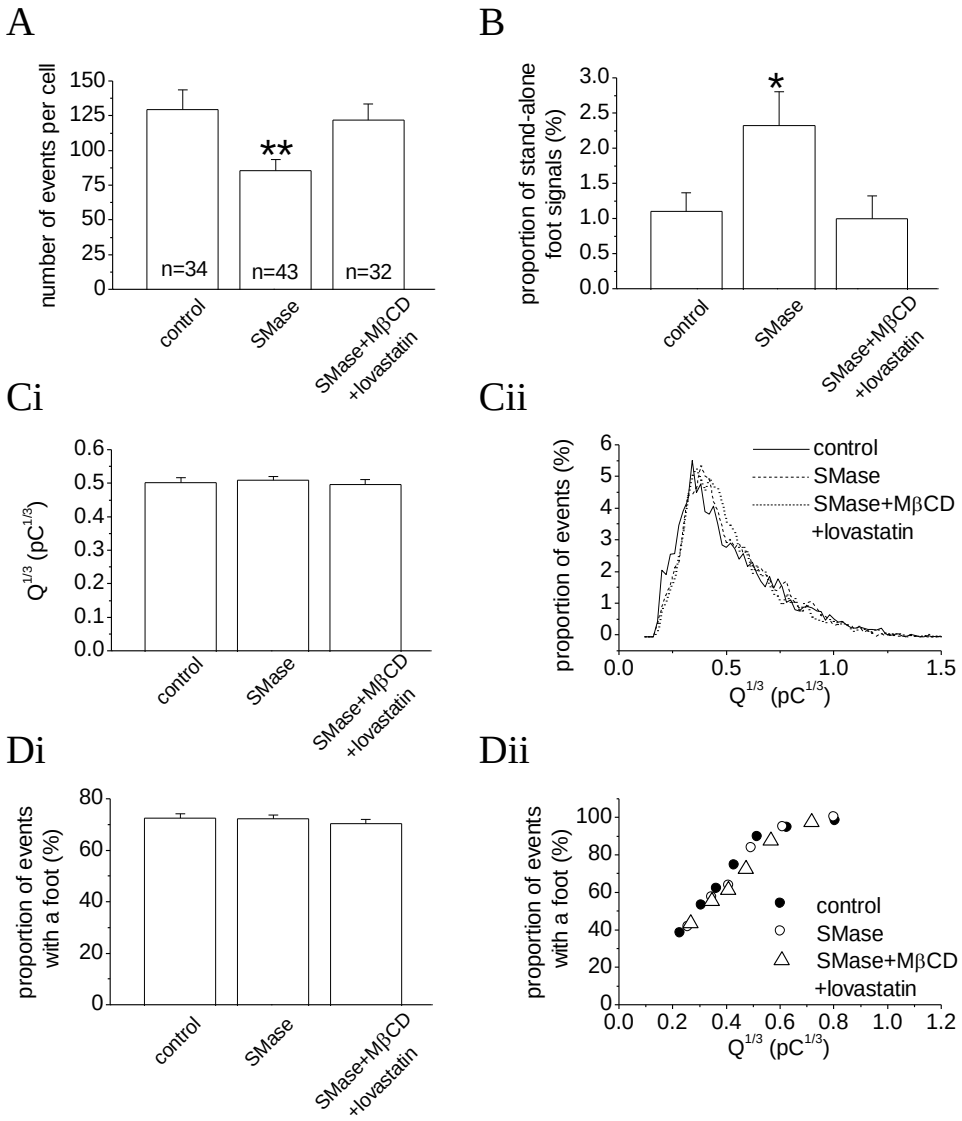

Figure 3.11 Effects of SMase (0.1U overnight) and SMase+MβCD+lovastatin (5μM lovastatin and 0.1U SMase overnight prior to 5mM MβCD for 1hr) on the number of events per cell, the proportion of "stand-alone foot" signals, the Q of the LDCGs, and the proportion of events with a foot. (A) SMase caused a significant reduction in the number of events per cell, but this effect was not detected with SMase+MβCD+lovastatin. (B) SMase increased the proportion of "stand-alone foot" signals but this effect was eliminated by SMase+MβCD+lovastatin. SMase and SMase+MβCD+lovastatin did not change Q (C) or the proportion of events with a foot (D). In (A-D), data were generated from 34 control cells (4,445 events), 43 cells treated with SMase (3,749 events), 32 cells treated with SMase+MβCD+lovastatin (3,942 events). Each data point in (Dii) was averaged from 600 events.

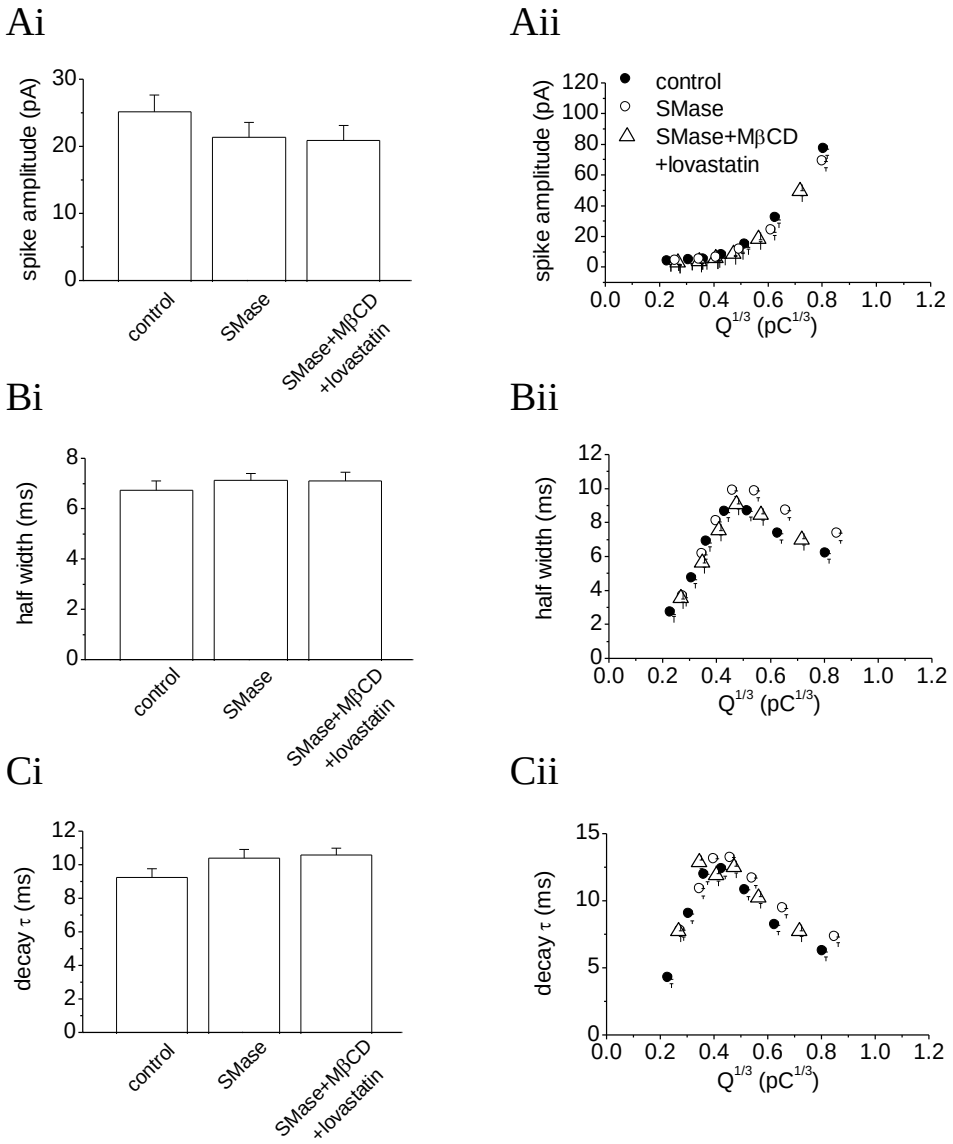

Figure 3.12 SMase (0.1U overnight) and SMase+MβCD+lovastatin (5μM lovastatin and 0.1U SMase overnight prior to 5mM MβCD for 1hr) did not affect the different kinetic parameters of the spike. Plots of the spike amplitude, half width, and decay τ for the mean cellular value (Ai, Bi and Ci) and at different values of $Q^{1/3}$(Aii, Bii and Cii) are shown. In (A-C), data were generated from 34 control cells (4,445 events), 43 cells treated with SMase (3,749 events), 32 cells treated with SMase+MβCD+lovastatin (3,942 events). Each data point in (Dii) was averaged from 600 events.

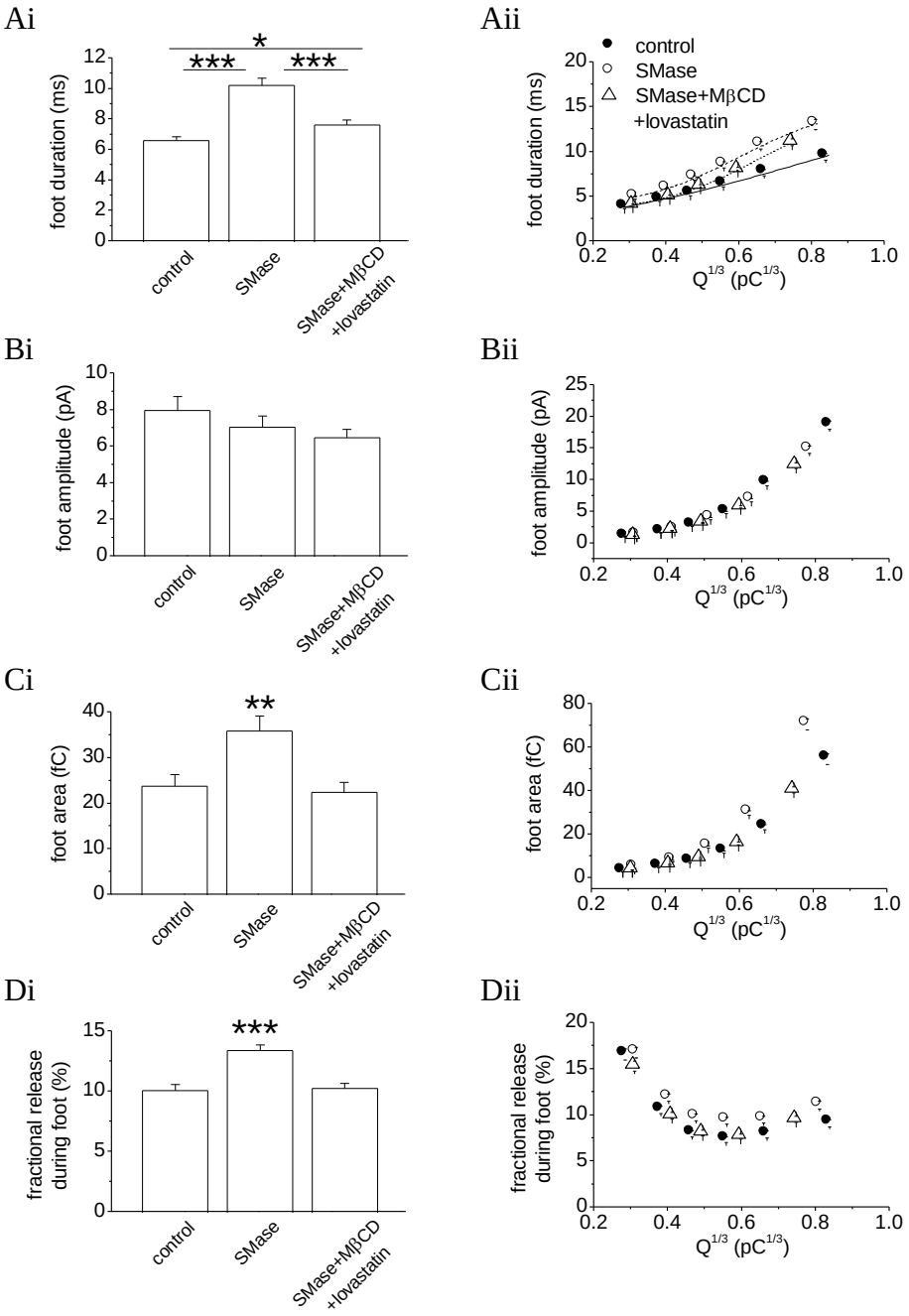

Figure 3.13 Effects of SMase (0.1U overnight) and SMase+MβCD+lovastatin (5μM lovastatin and 0.1U SMase overnight prior to 5mM MβCD for 1hr) on the foot duration, the foot area and the fractional release during foot. (A) SMase increased the foot duration, but this effect was partially reduced by SMase+MβCD+lovastatin. (B) SMase or SMase+MβCD+lovastatin had no significant effect on the foot amplitude. The increase in foot area (C) and the fractional release during foot (D) by SMase were reversed by SMase+MβCD+lovastatin. In (A-D), data were generated from 34 control cells (3,226 events), 43 cells treated with SMase (2,752 events), 32 cells treated with SMase+MβCD+lovastatin (2,816 events). Each data point in (Aii, Bii, Cii and Dii) was averaged from 500 events.

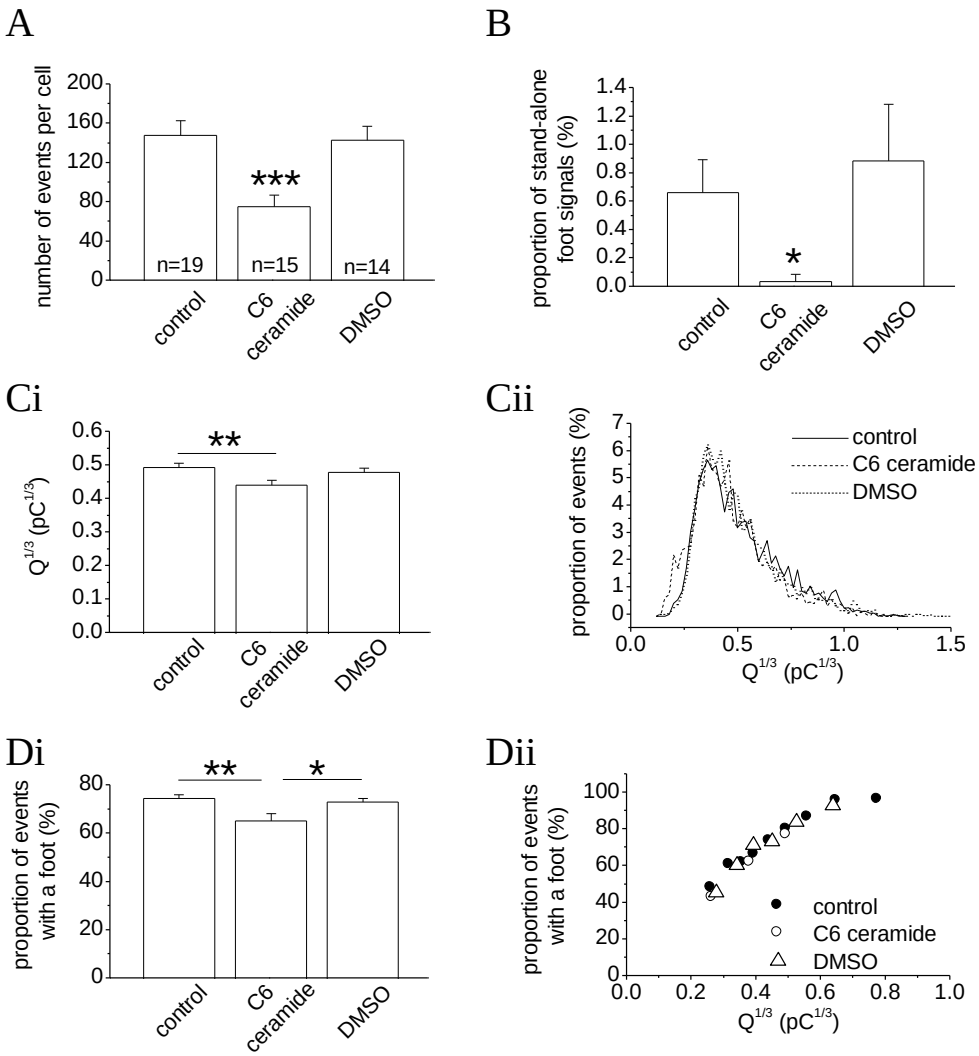

Figure 3.14 Effects of C6 ceramide (5μM for 1hr) and DMSO (0.1% for 1hr) on the number of events per cell, the proportion of "stand-alone foot" signals, the Q of the LDCGs, and the proportion of events with a foot. (A) C6 ceramide, but not DMSO, caused a significant reduction in the number of events per cell. (B) C6 ceramide decreased the proportion of "stand-alone foot" signals significantly, but DMSO had no effect. (C) C6 ceramide but not DMSO significantly decreased Q. As is shown in (Cii), there was an increase of proportion of events at the $Q^{1/3}$ range between 0.15-0.25$pC^{1/3}$, and a slight decrease at between 0.6-1.0 $pC^{1/3}$ with C6 ceramide. (D) C6 ceramide significantly decreased the proportion of events with a foot for the mean value of $Q^{1/3}$, but DMSO did not affect it. There was no dramatic reduction of the proportion of events with a foot for C6 ceramide treatment at matched values of $Q^{1/3}$ (Dii). In (A-D), data were generated from 19 control cells (2,845 events), 15 cells treated with C6 ceramide (1,155 events), and 14 cells treated with DMSO (2,030 events). Each data point in (Dii) was averaged from 300 events.

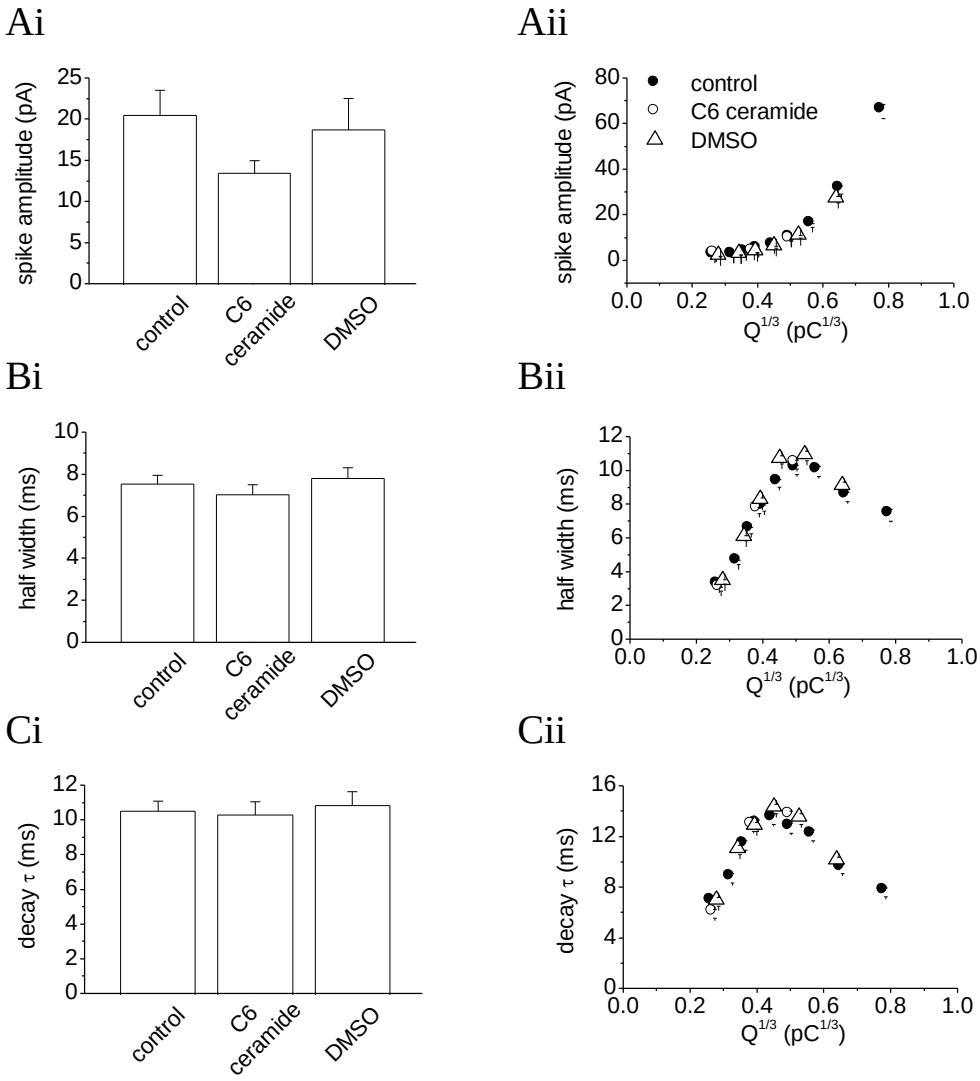

Figure 3.15 C6 ceramide (5μM for 1hr) and DMSO (0.1% for 1hr) did not affect the different kinetic parameters of the spike at matched values of $Q^{1/3}$. Plots of the spike amplitude, half width, and decay τ for the mean cellular value (Ai, Bi and Ci) and at different values of $Q^{1/3}$(Aii, Bii and Cii) are shown. In (A-C), data were generated from 19 control cells (2,845 events), 15 cells treated with C6 ceramide (1,155 events), and 14 cells treated with DMSO (2,030 events). Each data point in (Dii) was averaged from 300 events.

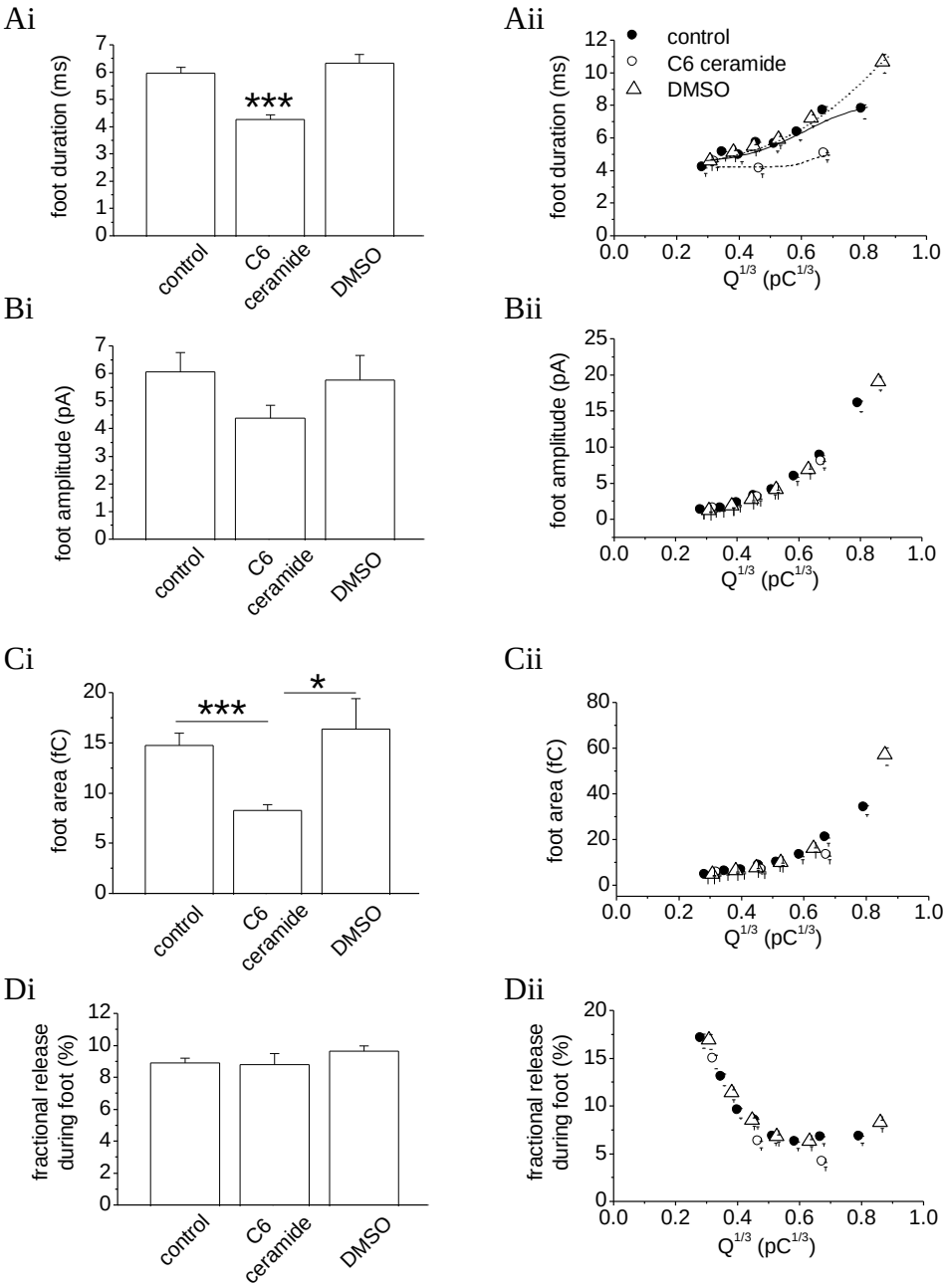

Figure 3.16 Effects of C6 ceramide (5μM for 1hr) and DMSO (0.1% for 1hr) on the foot duration, the foot area and the fractional release during foot. (A) C6 ceramide decreased the foot duration significantly, and this reduction was distinguishable at matched values of $Q^{1/3}$ (Ai). DMSO did not affect foot duration. (B) C6 ceramide and DMSO had no significant effect on the foot amplitude. (C) The foot area was decreased by C6 ceramide, but not by DMSO. (D) The fractional release during foot was not affected by C6 ceramide or DMSO for the mean cellular value (Di), but there was a trend of reduction for C6 ceramide at matched values of $Q^{1/3}$ (Dii). In (A-D), data were generated from 19 control cells (2,130 events), 15 cells treated with C6 ceramide (779 events), and 14 cells treated with DMSO (1,503 events). Each data point in (Aii, Bii, Cii and Dii) was averaged from 250 events.

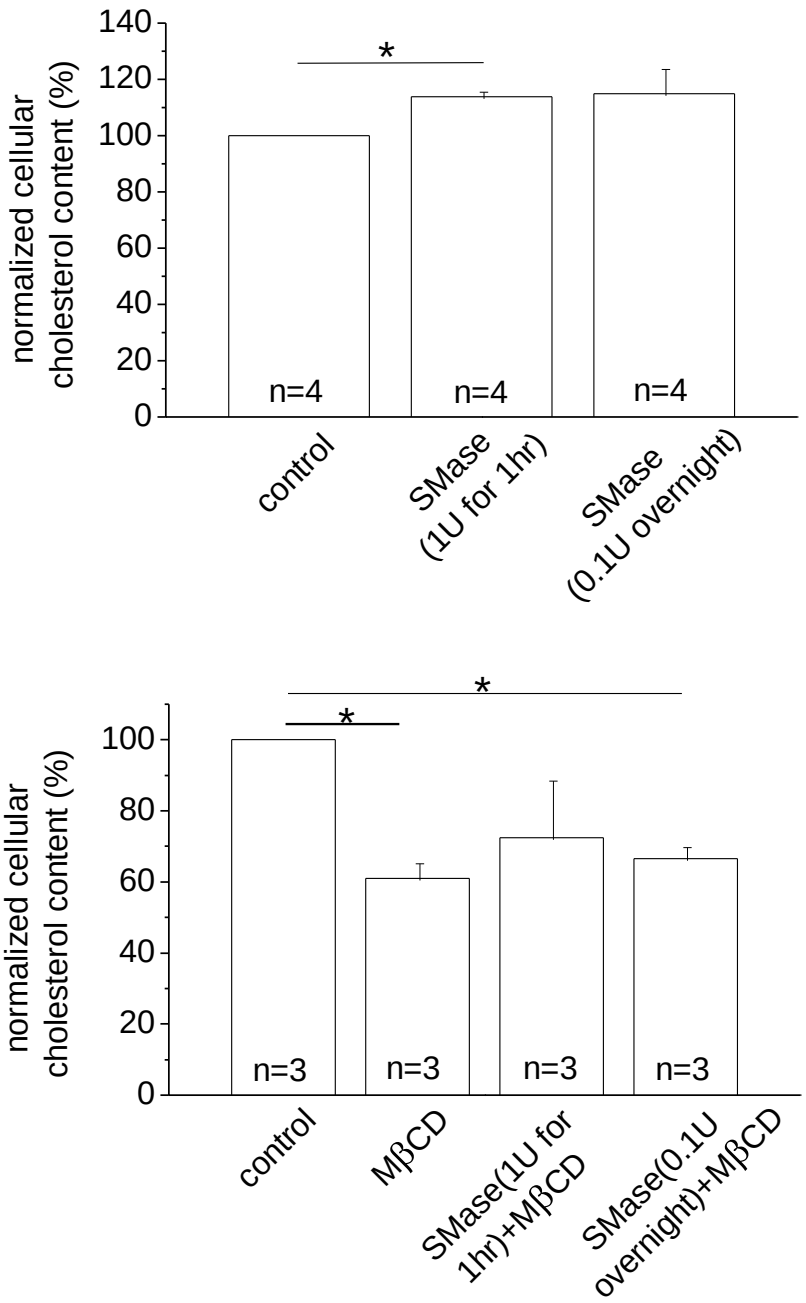

Figure 3.17 Effects of SMase (1U for 1hr) and SMase (0.1U overnight) on cellular less organized cholesterol content in rat chromaffin cells. (A) SMase increased the cellular less organized cholesterol content. Noticeably, there was no significant difference between SMase (1U for 1hr) and SMase (0.1U overnight). The results were obtained from 4 experiments. (B) MβCD, SMase (1U for 1hr)+MβCD and SMase (0.1U overnight)+MβCD caused a reduction in cellular less organized cholesterol content, but no significant difference was observed between these three treatment groups. The results were obtained from 3 experiments. In each experiment, cholesterol content was normalized to its corresponding control.

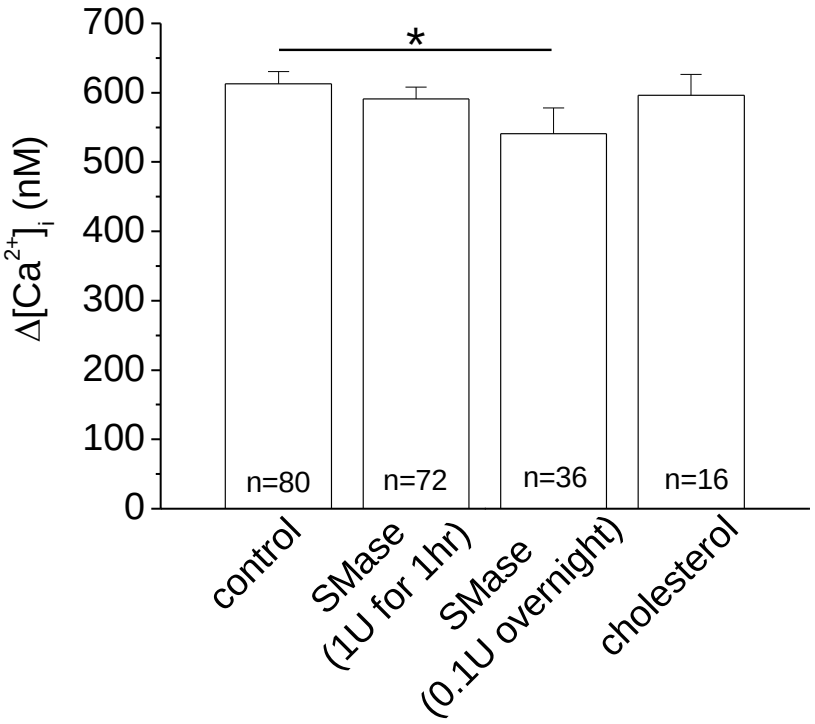

Figure 3.18 Effects of SMase (1U for 1hr), SMase (0.1U overnight) and cholesterol overload on the changes in $[Ca^{2+}]_i$. SMase (1U for 1hr) and cholesterol overload did not reduce the $\Delta[Ca^{2+}]_i$ significantly. SMase (0.1U overnight) caused a slight but significant decrease in $\Delta[Ca^{2+}]_i$. Data were obtained from 80 control cells, 72 cells treated with SMase (1U for 1hr), 36 cells treated with SMase (0.1U overnight) and 16 cells treated with cholesterol.

References

Elhamdani, A., Palfrey, H. C. and Artalejo, C. R. (2001) Quantal size is dependent on stimulation frequency and calcium entry in calf chromaffin cells. *Neuron,* **31,** 819-830.

Fernandez-Chacon, R. and Alvarez de Toledo, G. (1995) Cytosolic calcium facilitates release of secretory products after exocytotic vesicle fusion. *FEBS Lett,* **363,** 221-225.

Goni, F. M. and Alonso, A. (2009) Effects of ceramide and other simple sphingolipids on membrane lateral structure. *Biochim Biophys Acta,* **1788,** 169-177.

Scepek, S., Coorssen, J. R. and Lindau, M. (1998) Fusion pore expansion in horse eosinophils is modulated by Ca^{2+} and protein kinase C via distinct mechanisms. *EMBO J,* **17,** 4340-4345.

Tang, K. S., Wang, N., Tse, A. and Tse, F. W. (2007) Influence of quantal size and cAMP on the kinetics of quantal catecholamine release from rat chromaffin cells. *Biophys J,* **92,** 2735-2746.

Wang, N., Kwan, C., Gong, X., de Chaves, E. P., Tse, A. and Tse, F. W. (2010) Influence of cholesterol on catecholamine release from the fusion pore of large dense core chromaffin granules. *J Neurosci,* **30,** 3904-3911.

Xia, F., Leung, Y. M., Gaisano, G. et al. (2007) Targeting of voltage-gated K^+ and Ca^{2+} channels and soluble N-ethylmaleimide-sensitive factor attachment protein receptor proteins to cholesterol-rich lipid rafts in pancreatic alpha-cells: effects on glucagon stimulus-secretion coupling. *Endocrinology,* **148,** 2157-2167.

Xia, F., Xie, L., Mihic, A., Gao, X., Chen, Y., Gaisano, H. Y. and Tsushima, R. G. (2008) Inhibition of cholesterol biosynthesis impairs insulin secretion and voltage-gated calcium channel function in pancreatic beta-cells. *Endocrinology,* **149,** 5136-5145.

Chapter 4: Discussion

The results presented in Chapter 3 can be summarized as follows. My two SMase treatments caused similar reductions of cellular SM content (by ~20% (1U for 1hr) and ~14% (0.1U for overnight) respectively). With elevated extracellular $[K^+]$ as the trigger for exocytosis, both SMase treatments led to a slight inhibition of exocytosis and a clear increase in the proportion of "stand-alone foot" signals as well as the duration of the prespike foot signal; in contrast, Q, the main spike kinetics and foot amplitude were unaffected. These overall effects of SMase on quantal release were mimicked by cholesterol overload, but not by C6 ceramide overload, and could be reduced by cholesterol extraction. Because the rise in $[Ca^{2+}]_i$ that triggered exocytosis might also regulate the quantal release kinetics, I examined whether it was affected by SMase treatment. It turned out that the $\Delta[Ca^{2+}]_i$ stimulated by elevating extracellular $[K^+]$ was slightly decreased following SMase treatment. Interestingly, the effects of 1U SMase treatment for 1hr on quantal release and $\Delta[Ca^{2+}]_i$ were less robust than those of a 15~20-fold longer-time treatment of SMase with a 10-fold less concentration (0.1U SMase overnight), yet the two SMase treatments caused a similar small increase in the cellular level of readily detectable cholesterol.

In the following sections I will first focus my discussion on the following issues.

(1) Why did SMase treatment lead to a very modest drop in cellular SM content?

(2) What are the possible mechanisms underlying the effects of SMase on quantal release kinetics?

(3) and (4) What are the contributions of ceramide and a change in the triggering $[Ca^{2+}]$ to the change in quantal release?

(5) What is the physiological and pathological significance of this study?

I. Why did SMase treatment lead to a very modest drop in cellular SM content?

SM is not only located in the plasma membrane, but also widely distributed inside the cell. For example, through SMase gene transfection in MCF7 breast cancer cells, fusion proteins contained in the vectors selectively targeted SMase to individual cellular compartments, including the inner leaflet of the plasma membrane, the cytoplasm, the mitochondria, the ER, the Golgi apparatus, and the nucleus. As a result of SM hydrolysis, elevation of the cellular ceramide level was observed in each targeted compartment, indicating the presence of intracellular pools of SM (Birbes *et al.* 2001). Endosomes, which are responsible for the internalization and recycling of most of the SM in the plasma membrane, were found to contain similar amounts of SM to the plasma membrane in rat liver cells (~17% phospholipids) (Evans & Hardison 1985). SM was also reported to exist in the chromaffin granule membrane (Buckland *et al.* 1978).

In my experiments, the treatment with 1U SMase for 1hr and 0.1U SMase overnight resulted in ~20% and ~14% reduction in cellular SM content of chromaffin cells respectively. SMase in the culture medium can only catalyze the hydrolysis of SM in the extracellular leaflet of the plasma membrane, rather than exert its function inside the cell, because plasma membrane is impermeable to this 34kDa enzyme (Tamura *et al.* 1992). Almost all SM of the plasma membrane resides in the extracellular leaflet, therefore this localized action of SMase can perturb the SM of plasma membrane (where exocytosis occurs) to a large degree without disturbing the cytosolic SM. That also explains why the relatively high concentration of SMase treatment did not lead to a very dramatic drop in cellular SM content.

II. What are the possible mechanisms underlying the effects of SMase on quantal release kinetics?

In order to better interpret the results of the studies on kinetic parameters of quantal release, especially the foot signal, a brief introduction to the fusion process and the structure of the fusion pore is necessary. The core of the molecular machinery for fusion is the formation of a SNARE complex, which serves as a bridge between a primed LDGC (Sugita 2008) and the plasma membrane. The SNARE complex consists of three proteins: synaptosome-associated protein of 25kDa (SNAP-25) and syntaxin on the plasma membrane, and synaptobrevin on the LDGC membrane. Following a rise in $[Ca^{2+}]_i$, which is sensed by synaptotagmin, a key Ca^{2+} sensor on the LDGC membrane, SNARE complex zippering pulls the opposing membranes together, leading to the formation of the fusion pore (Jackson & Chapman 2006). It is not clear whether the SNARE complex also contributes to the dilation of the fusion pore. Although the fusion pore is an important component in the exocytosis machinery, its structure is not completely understood. Two models of the initial fusion pore have been proposed depending on whether the wall is proteinaceous or lipidic. The model of proteinaceous fusion pore postulates that the pore is analogous to a gap junction-like channel lined with entirely protein (probably the SNARE proteins). The model of lipidic fusion pore predicts that the hemi-fusion of the opposing cytosolic leaflets is first formed by the action of the SNARE complex, and then the extracellular leaflet of the plasma membrane merges with the luminal leaflet of the granule membrane, so that the wall of the fusion pore is essentially lipidic. No matter in which category the initial fusion pore falls, adjacent lipid molecules are definitely needed for the expansion of the pore, otherwise it may close, giving rise to a “stand-alone foot” signal (Jackson & Chapman 2006, Jackson & Chapman 2008). According to a typical amperometric signal recorded from a chromaffin cell as shown in Fig. 1.2A, the amplitude of the foot signal typically increases gradually rather than in a

step-wise fashion, indicating a continuous incorporation of lipid during the semi-stable state of fusion pore. The diameter of initial fusion pore is 1-2nm (Rahamimoff & Fernandez 1997). To form such a small pore, the sharp negative curvature of the cytosolic side (i.e. the continuous membrane made by the fusion of the cytosolic leaflet of plasma membrane and cytosolic leaflet of granule membrane), as well as the sharp positive curvature of the extracellular side (i.e. the continuous membrane made by the fusion of the extracellular leaflet of plasma membrane and luminal side of granule membrane), are required (Fig. 4.1). Negative curvature is defined as phospholipid heads being concave toward the water environment, whereas positive curvature is convex toward it. Using whole-cell dialysis of a Ca^{2+}-buffered internal solution as the trigger for exocytosis in rat chromaffin cells, Wang *et al.* (2010) found that after inhibition of cholesterol synthesis, an oversupply of cholesterol (for 1hr) could still increase the foot duration and the proportion of "stand-alone foot" signal, reflecting the reluctance of fusion pore dilation, while cholesterol extraction (for 1hr) showed opposite effects. Moreover, acute extraction (~5min) of cholesterol from the cytosolic leaflets, rather than from the extracellular leaflet of the plasma membrane, decreased the foot duration and the proportion of "stand-alone foot" signal. According to that study, the ability of cholesterol in the cytosolic leaflets of the semi-stable fusion pore to hinder its expansion probably involved three properties of cholesterol molecules. First, the viscosity of the lipid membrane might be enhanced by cholesterol, and this is expected to inhibit the incorporation of lipid molecules into the initial fusion pore. Second, cholesterol can slightly increase the stiffness of a lipid monolayer (i.e. make it harder to bend). Third, similar to a cone-shaped lipid, cholesterol is postulated to help form the negative curvature of the cytosolic leaflet by intercalating between the acyl tails of phospholipids (Fig. 4.1 inset). Cholesterol was indeed reported to impede the transition from hemifusion to full fusion between phospholipid bilayer vesicles (Garcia *et al.* 2001).

MβCD is a cyclic oligosaccharide, composed of seven glucose units. Because of its high affinity for cholesterol, MβCD is frequently used to remove cholesterol from the extracellular leaflet of the plasma membrane by incorporating it into the ring structure of MβCD, while MβCD saturated with cholesterol is also efficient in overloading cholesterol to cellular membranes (Zidovetzki & Levitan 2007). In my study, MβCD was employed to overload and extract cholesterol from the plasma membrane of rat chromaffin cells. With high [K^+] as the trigger for exocytosis, SMase treatment caused selective effects that are similar to cholesterol overload on two kinetic parameters of quantal release: an increase in the foot duration and the proportion of "stand-alone foot" signal. Moreover, the simultaneous treatment of SMase and cholesterol has a roughly additive effect. Most importantly, the changes in kinetic parameters resulting from SMase can be reduced by cholesterol extraction. My overall results suggest that SMase treatment liberated some cholesterol that previously interacted tightly with SM in lipid rafts, and the liberated cholesterol in turn stabilized the semi-stable fusion pore. The liberation of cholesterol resulting from the action of SMase was previously confirmed by a larger efflux of [^{3}H] cholesterol mediated by MβCD (Subbaiah *et al.* 2003, Tepper *et al.* 2000, Haynes *et al.* 2000). As mentioned above, cholesterol in the cytosolic leaflets might be particularly important for constraining the fusion pore before the onset of rapid dilation; thus it is probable that the freed cholesterol molecules in the extracellular leaflet of the plasma membrane flip to the cytosolic side and therein stabilize the fusion pore. Cholesterol can undergo a relatively rapid transbilayer movement with a half-time of 50min in human erythrocyte membrane (Brasaemle *et al.* 1988). In this study, 0.1U SMase overnight caused larger alteration in foot signal and "stand-alone foot" signal than 1U SMase for 1hr, therefore a cholesterol assay detecting cellular free cholesterol was performed to test whether the two procedures actually changed the amount of free cholesterol to different levels. In the cholesterol assay, chromaffin cells were first lysed by RIPA buffer

(which might not disrupt lipid rafts efficiently), and then the cholesterol and cholesterol esters in the lysate were quantified with the Amplex Red cholesterol assay kit. This assay is based on the fluorescent detection of H_2O_2, which is produced during the oxidation of cholesterol by cholesterol oxidase. According to Lange and Steck (2008), when a cholesterol molecule is interacting tightly with SM, whose phosphocholine head provides a molecular umbrella that can shield the cholesterol molecule from the aqueous phase, the shielded cholesterol may be less accessible to cholesterol oxidase. Therefore, with my protocol the detected cholesterol probably represents the less organized cholesterol. Compared to controls, both SMase treatments increased the cellular cholesterol content by ~15%, which is consistent with the liberation of more "detectable" cholesterol following the disruption of the tight interaction with SM. However, there was no difference in the amount of freed cholesterol between these two treatments, and also 0.1U of SMase overnight did not cause more SM to be hydrolyzed than 1U SMase for 1hr. Therefore it is probable that the more robust effect on quantal release resulting from the longer treatment with 10-fold lower concentration is attributable to the more time available for the liberated cholesterol to flip to the cytosolic leaflet (and perhaps also redistribute elsewhere). In my study, 1U SMase for 1hr with simultaneous cholesterol extraction essentially eliminated the effect of SMase on foot signals and "stand-alone foot" signals. Under this condition, as soon as cholesterol is liberated in the extracellular leaflet of the plasma membrane, it might be rapidly extracted by MβCD, such that it has less chance to flip. On the other hand, 0.1U SMase overnight allowed more time for the freed cholesterol to flip to the cytosolic leaflet where MβCD was not accessible; this may explain why even the inhibition of cholesterol synthesis, followed by cholesterol extraction, failed to bring the foot duration back to normal (although the effect of SMase on increasing the proportion of "stand-alone foot" signal was essentially eliminated).

III. What is the contribution of ceramide to the change in quantal release?

Following the hydrolysis of SM catalyzed by SMase, ceramide is generated in the extracellular leaflet of the plasma membrane as a by-product. Ceramide and its metabolites such as sphingosine and sphingosine-1-phosphate are known for their potential roles in signalling transduction leading to growth arrest, differentiation and apoptosis (Riboni *et al.* 1997). Ceramide can activate protein kinases such as PKC as well as some protein phosphatases (Ruvolo 2003). Ceramide was also reported to stimulate adenylyl cyclase (AC) in human embryonic kidney cells (Bosel & Pfeuffer 1998). The activated AC could catalyze the conversion of adenosine 5'-triphosphate (ATP) to cyclic adenosine 3',5'-monophosphate (cAMP, that was reported to shorten the foot duration in the large-Q granules in rat chromaffin cells (Tang et al. 2007a)). In chromaffin cells, activation of PKC was reported to increase exocytotic events (Gillis et al. 1996) and narrow the main spike leading to smaller Q when $[Ca^{2+}]_i$ was elevated by permeabilizing the cell with a detergent (digitonin) (Graham et al. 2000). According to the cofactor requirements, PKC isoforms are classified into three groups: classical PKC isoform (α, β and γ), which is activated by Ca^{2+} and DAG; novel PKC isoform (δ, ε, η and θ), which requires DAG for activation; and atypical PKC isoform (ζ and ι/λ), which does not respond to either Ca^{2+} or DAG (Morgan *et al.* 2005). Selective activation of PKC isoforms depends on the type of cell studied. For example, PKCα was found to be selectively activated by ceramide in renal mesangial cells (Huwiler et al. 1998). In vascular smooth muscle cells, PKCζ was reported to be activated by ceramide (Fox et al. 2007), and Bourbon (2002) proposed that ceramide-mediated growth arrest may be due to the negative regulation of Akt activity by PKCζ (fully functional Akt is able to induce protein synthesis of many pro-mitogenic transcription factors). The PKC isoform involved in the ceramide-mediated signalling pathway in chromaffin cells has not yet been identified. It is noteworthy that in studies focusing on the effect of PKC on secretion, phorbol ester (the analogue of

DAG) was used as the stimulator of PKC, confirming that classical and novel isoforms can influence secretion, but whether atypical isoforms have similar effects still remains unknown. Therefore, in my study, external ceramide was overloaded on chromaffin cells in order to test the impact of this by-product of SMase on quantal release kinetics. Due to the very low aqueous solubility of ceramides with longer acyl chains, C6 ceramide, which can indeed activate PKC, was employed. My data showed that after C6 ceramide treatment, not only was the number of amperometric signals reduced, but there was a larger fraction of events with the lowest range of $Q^{1/3}$ which led to a smaller average cellular value of $Q^{1/3}$ compared to controls. At matched values of $Q^{1/3}$, the kinetic parameters of the main spike were unaffected, but the foot duration became shorter and the proportion of "stand-alone foot" signals was obviously decreased. These findings suggest that C6 ceramide selectively destabilizes the semi-stable fusion pore. Therefore the possibility that the increase in ceramide resulting from SMase treatment affected quantal release through classical and novel PKC isoforms in chromaffin cells could be essentially ruled out. The effects of C6 ceramide on the foot signals were opposite to those of SMase treatment, and are consistent with the scenario that C6 ceramide (because of its inverted-cone shape (Sot *et al.* 2005)) endows positive curvature to the extrcellular leaflet of plasma membrane at the fusion pore (Fig. 4.2A), while, C6 ceramide probably does not increase membrane viscosity like cholesterol. In addition, it is also possible that ceramide activates AC, and the generated cAMP destabilizes the initial fusion pore, although in my study, the foot duration was shortened over essentially the entire range of $Q^{1/3}$. Unlike C6 ceramide, SMase-generated ceramide always has a long acyl chain, thus it can promote negative curvature in one monolayer (Sot et al. 2005) (Fig. 4.2B). If this physical property was responsible for the stabilization of fusion pore brought about by SMase treatment, it could not explain why MβCD reduced the effects, for β-cyclodextrin has little power to extract ceramide (Singh & Kishimoto 1983). Furthermore, SMase treatment did not change Q and main

spike kinetics, so it is unlikely that the ceramide with long acyl chains has a major impact on quantal release via PKC. In conclusion, the effects of SMase on the kinetics of the fusion pore are unlikely to be mediated via the by-product, ceramide.

IV. What is the contribution of a change in the triggering [Ca^{2+}] to the change in quantal release?

In comparison to control cells, fewer exocytotic events were observed in SMase-treated cells. Specifically, 0.1U SMase overnight significantly decreased this parameter to 70% of control. The inhibition of exocytosis by SMase was consistent with the dose-dependent inhibition of fusion between sea urchin cortical vesicles, which was accompanied by a reduction in their sensitivity to Ca^{2+} as a trigger for fusion (Rogasevskaia & Coorssen 2006). As the by-product of SM hydrolysis, ceramide was also demonstrated to attenuate VGCC activity in rat adrenal chromaffin cells (Liu *et al.* 2001). Ca^{2+} is a robust trigger for the secretory machine of neurotransmitter and hormone release. $[Ca^{2+}]_i$ has a positive correlation with the amount of released catecholamine from individual cells as well as individual granules (Michelena *et al.* 1993, Elhamdani et al. 2001), and can accelerate the fusion pore expansion in a variety of cell types (Scepek et al. 1998, Fernandez-Chacon & Alvarez de Toledo 1995). In my study, fura-2 was employed to quantify the change in $[Ca^{2+}]_i$. Consistent with the trend in number of exocytotic events, both SMase treatments caused a slight reduction in $\Delta[Ca^{2+}]_i$, and with 0.1U SMase overnight the drop was larger and statistically significant .

To minimize any secondary effect on quantal release kinetics which might arise from the change in $[Ca^{2+}]_i$, a postdoctoral fellow in our lab, Dr. Xiandi Gong, employed whole-cell dialysis of a Ca^{2+}-buffered solution ($[Ca^{2+}]_i$ = ~0.5μM) to trigger quantal catecholamine release from rat chromaffin cells (thus bypassing any possible effect of SMase on calcium channels). His data (not shown in this thesis) indicated that SMase did not

alter the overall rate of exocytosis in 5 minutes when $[Ca^{2+}]_i$ was clamped, and more importantly, SMase still prolonged the foot duration and increased the proportion of "stand-alone foot" signals, whereas other kinetic parameters remained unchanged —— the same as my results. In my study, cholesterol overload also showed a trend to inhibit exocytosis, but the $\Delta[Ca^{2+}]_i$ was not significantly different from controls. The mechanism of inhibition is not clear, but may need a longer duration to develop, considering 0.1U SMase overnight did not generate more ceramide or liberate more cholesterol, but attenuated the exocytosis more than 1U SMase for 1hr.

V. Physiological significance

Exocytosis is a vital process mediating the cellular secretion of neurotransmitters and hormones stored in vesicles and dense core granules. Even subtle changes in exocytosis could have a huge influence on the efficiency of communication between neurons and the regulation of the body's response to hormone secretion. A previous study from our lab showed that pertubation of cholesterol in the membrane could regulate fusion pore kinetics. SM hydrolysis can regulate the proportion of the structured- and free-cholesterol. My thesis has raised the possibility that free-cholesterol could stabilize the fusion pore, for it increased the proportion of "stand-alone foot" signal and the foot duration. The flickering and closure of a semi-stable fusion pore gives rise to a "stand-alone foot" signal; if this type of exocytosis leads to incomplete discharge of the vesicular cargo, then the overall efficiency of exocytosis will be reduced. In addition, the slightly slower fusion pore may be functionally less significant for the endocrine output from a chromaffin cell, because it takes many seconds for the hormone to travel from the adrenal gland to the rest of the body. But in the synapse and autocrine/paracrine interactions, this issue can become a major one because the slow leakage of transmitters from a very small fusion pore is expected to lead to desensitization of postsynaptic receptors (Jackson & Chapman 2008).

Therefore, It raises the possibility that hypercholesterolemia is associated with an increased risk of neurological diseases. Niemann-Pick type A disease, resulting from the deficiency of aSMase, can cause severe neurodegenerative disorders in infancy (Kolodny 2000); Niemann-Pick type C 1 (NPC1) disease, in which the functional NPC1 protein is lacking, can result in gross abnormalities in the distribution of cholesterol in different cellular compartments of neurons as well as neurological symptoms (Karten *et al.* 2003).

VI. Conclusions

The work of this thesis focuses on the effects of SM hydrolysis in the plasma membrane of rat adrenal chromaffin cells on quantal release. Similar to cholesterol overload, SMase treatment significantly increased the proportion of “stand-alone foot” signals and duration of the prespike foot signals, while Q, main spike kinetics and foot amplitude were unaffected. Specifically, 0.1U SMase overnight had a more dramatic effect than 1U SMase for 1hr. The effects of 1U SMase for 1hr could be eliminated by a cholesterol extractor, whereas those of 0.1U SMase overnight, especially the foot duration, could only be partially reduced by both cholesterol synthesis inhibition and extraction. My SM assay and cholesterol assay showed that 0.1U SMase overnight did not hydrolyze more SM or liberate more free cholesterol than 1U SMase for 1hr. The last finding raises the possibility that the longer SMase treatment allowed for freed cholesterol to flip-flop to the cytosolic leaflet of the plasma membrane, where it was previously shown to be more important in stabilizing the semi-stable fusion pore. The by-product of SM hydrolysis, ceramide (at least the C6 version with an acyl chain shorter than those in cellular SM) simply could not mimic the effects of SMase on either type of foot signal. The reduction in the rate of exocytosis by both SMase treatments may involve a slightly lower elevation in $[Ca^{2+}]_i$. In summary, my data are consistent with the scenario that SMase treatment liberated cholesterol

molecules from a previously strong interaction with SM, and the liberated cholesterol molecules in turn redistributed to other sites (probably in the cytosolic leaflet) that can increase the persistence of the semi-stable fusion pore before the onset of rapid dilation.

VII. Future directions

To further explore the above scenario, the tracking of the flip-flop of cholesterol molecules between the two monolayers of the plasma membrane will be required. The role of ceramide with longer acyl chains (similar to those found in cellular SM) in quantal kinetics also needs to be clarified; at present, the loading efficiency of such molecules is the main hurdle. I am hopeful that in near future the advent of more biochemical, biophysical and molecular tools will allow us to explore such issues.

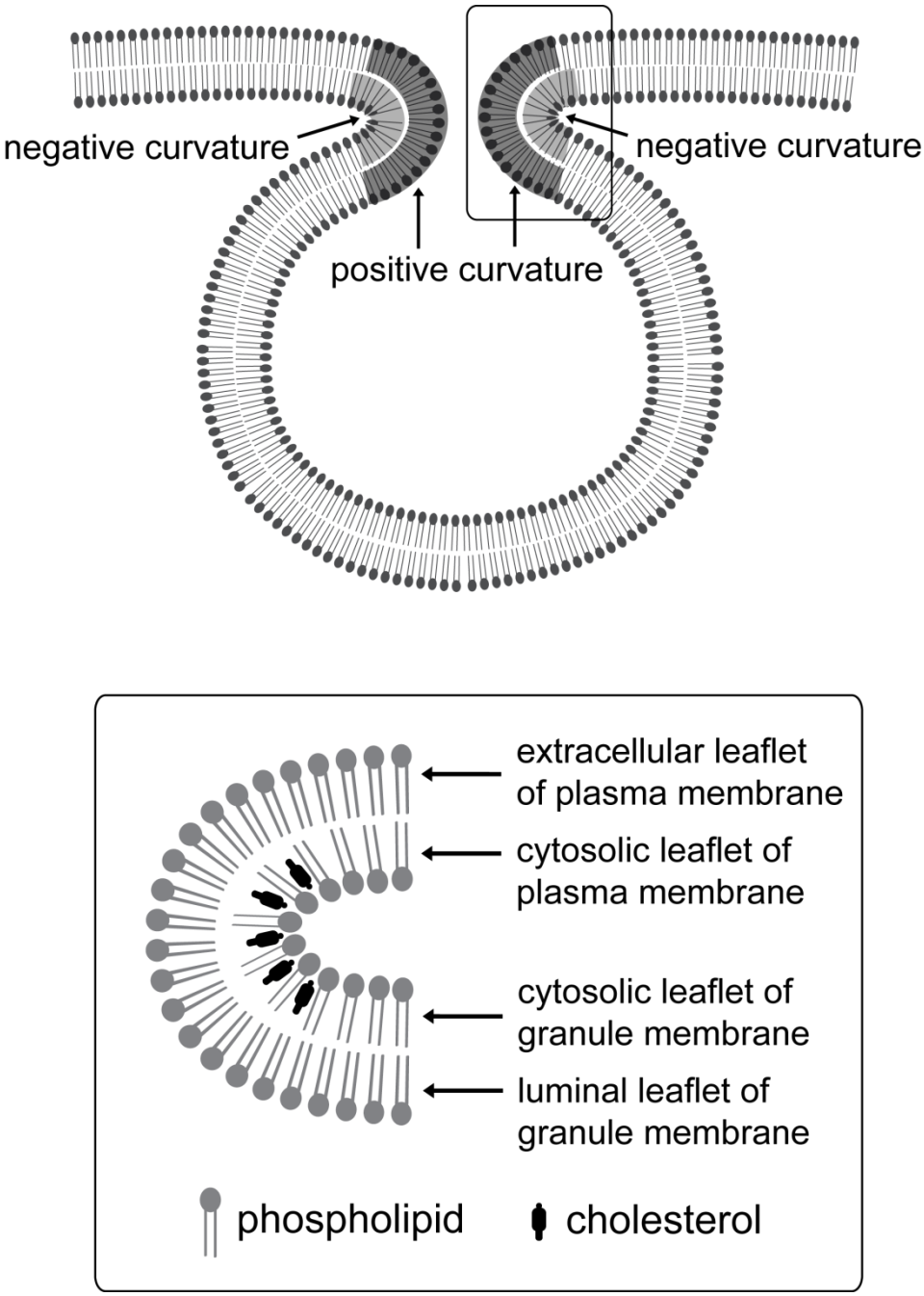

Figure 4.1 Structure of the fusion pore. Inset is the magnified image of the sharp curvatures formed during membrane fusion.

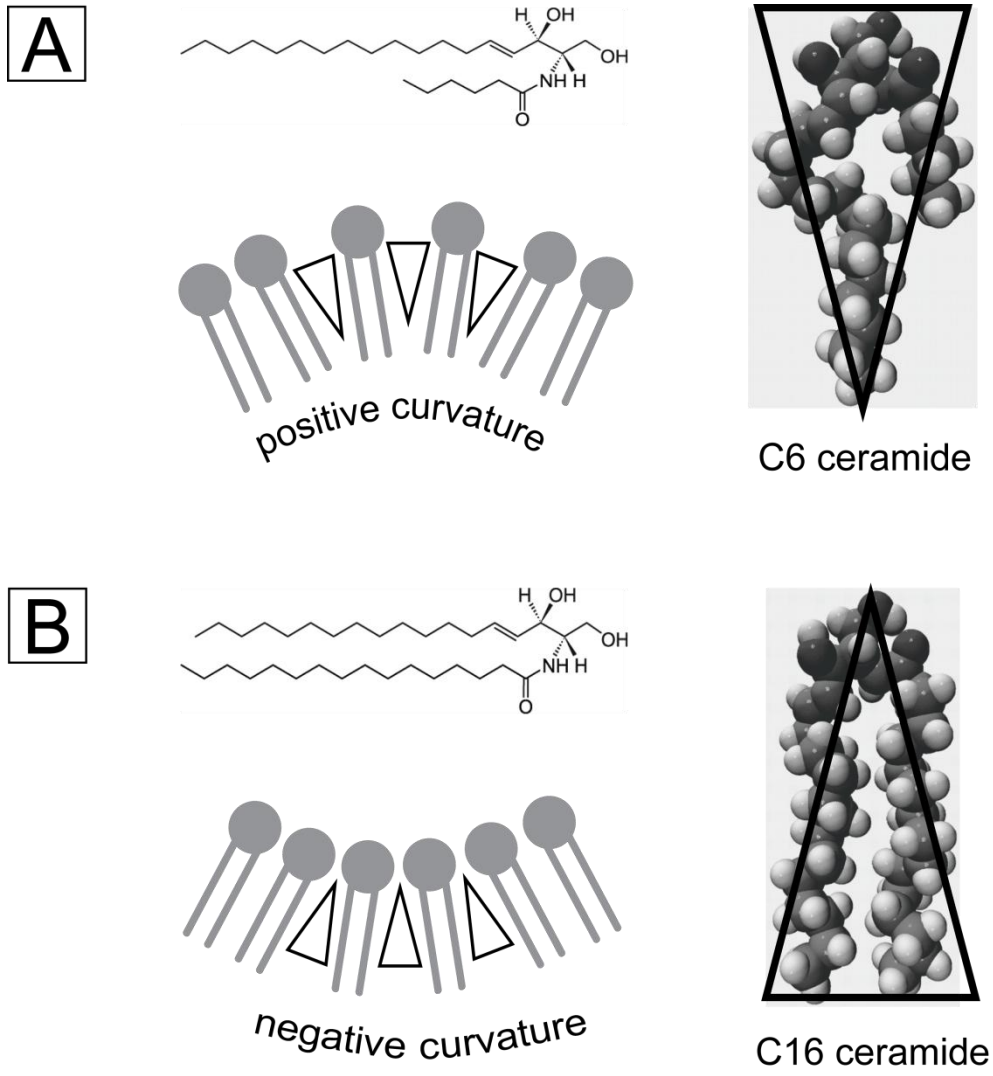

Figure 4.2 Comparison between C6 ceramide and C16 ceramide in their contribution to the lipid monolayer curvature. (A) the inverted-cone shaped C6 ceramide endows positive curvature. (B) the cone shaped C16 ceramide endows negative curvature.

References

Birbes, H., El Bawab, S., Hannun, Y. A. and Obeid, L. M. (2001) Selective hydrolysis of a mitochondrial pool of sphingomyelin induces apoptosis. *FASEB J,* **15,** 2669-2679.

Bosel, A. and Pfeuffer, T. (1998) Differential effects of ceramides upon adenylyl cyclase subtypes. *FEBS Lett,* **422,** 209-212.

Bourbon, N. A., Sandirasegarane, L. and Kester, M. (2002) Ceramide-induced inhibition of Akt is mediated through protein kinase Czeta: implications for growth arrest. *J Biol Chem,* **277,** 3286-3292.

Brasaemle, D. L., Robertson, A. D. and Attie, A. D. (1988) Transbilayer movement of cholesterol in the human erythrocyte membrane. *J Lipid Res,* **29,** 481-489.

Buckland, R. M., Radda, G. K. and Shennan, C. D. (1978) Accessibility of phospholipids in the chromaffin granule membrane. *Biochim Biophys Acta,* **513,** 321-337.

Elhamdani, A., Palfrey, H. C. and Artalejo, C. R. (2001) Quantal size is dependent on stimulation frequency and calcium entry in calf chromaffin cells. *Neuron,* **31,** 819-830.

Evans, W. H. and Hardison, W. G. (1985) Phospholipid, cholesterol, polypeptide and glycoprotein composition of hepatic endosome subfractions. *Biochem J,* **232,** 33-36.

Fernandez-Chacon, R. and Alvarez de Toledo, G. (1995) Cytosolic calcium facilitates release of secretory products after exocytotic vesicle fusion. *FEBS Lett,* **363,** 221-225.

Fox, T. E., Houck, K. L., O'Neill, S. M. et al. (2007) Ceramide recruits and activates protein kinase C zeta (PKC zeta) within structured membrane microdomains. *J Biol Chem,* **282,** 12450-12457.

Garcia, R. A., Pantazatos, S. P., Pantazatos, D. P. and MacDonald, R. C. (2001) Cholesterol stabilizes hemifused phospholipid bilayer vesicles. *Biochim Biophys Acta,* **1511,** 264-270.

Gillis, K. D., Mossner, R. and Neher, E. (1996) Protein kinase C enhances exocytosis from chromaffin cells by increasing the size of the readily releasable pool of secretory granules. *Neuron,* **16,** 1209-1220.

Graham, M. E., Fisher, R. J. and Burgoyne, R. D. (2000) Measurement of exocytosis by amperometry in adrenal chromaffin cells: effects of clostridial neurotoxins and activation of protein kinase C on fusion pore kinetics. *Biochimie,* **82,** 469-479.

Haynes, M. P., Phillips, M. C. and Rothblat, G. H. (2000) Efflux of cholesterol from different cellular pools. *Biochemistry,* **39,** 4508-4517.

Huwiler, A., Fabbro, D. and Pfeilschifter, J. (1998) Selective ceramide binding to protein kinase C-alpha and -delta isoenzymes in renal mesangial cells. *Biochemistry,* **37,** 14556-14562.

Jackson, M. B. and Chapman, E. R. (2006) Fusion pores and fusion machines in Ca^{2+}-triggered exocytosis. *Annu Rev Biophys Biomol Struct,* **35,** 135-160.

Jackson, M. B. and Chapman, E. R. (2008) The fusion pores of Ca^{2+}-triggered exocytosis. *Nat Struct Mol Biol,* **15,** 684-689.

Karten, B., Vance, D. E., Campenot, R. B. and Vance, J. E. (2003) Trafficking of cholesterol from cell bodies to distal axons in Niemann Pick C1-deficient neurons. *J Biol Chem,* **278,** 4168-4175.

Kolodny, E. H. (2000) Niemann-Pick disease. *Curr Opin Hematol,* **7,** 48-52.

Lange, Y. and Steck, T. L. (2008) Cholesterol homeostasis and the escape tendency (activity) of plasma membrane cholesterol. *Prog Lipid Res,* **47,** 319-332.

Liu, J., Jorgensen, M. S., Adams, J. M., Titlow, W. B., Nikolova-Karakashian, M. and Jackson, B. A. (2001) Ceramide modulates nicotinic receptor-dependent Ca^{2+} signaling in rat chromaffin cells. *J Neurosci Res,* **66,** 559-564.

Michelena, P., Garcia-Perez, L. E., Artalejo, A. R. and Garcia, A. G. (1993) Separation between cytosolic calcium and secretion in chromaffin cells superfused with calcium ramps. *Proc Natl Acad Sci U S A,* **90,** 3284-3288.

Morgan, A., Burgoyne, R. D., Barclay, J. W., Craig, T. J., Prescott, G. R., Ciufo, L. F., Evans, G. J. and Graham, M. E. (2005) Regulation of exocytosis by protein kinase C. *Biochem Soc Trans,* **33,** 1341-1344.

Rahamimoff, R. and Fernandez, J. M. (1997) Pre- and postfusion regulation of transmitter release. *Neuron,* **18,** 17-27.

Riboni, L., Viani, P., Bassi, R., Prinetti, A. and Tettamanti, G. (1997) The role of sphingolipids in the process of signal transduction. *Prog Lipid Res,* **36,** 153-195.

Rogasevskaia, T. and Coorssen, J. R. (2006) Sphingomyelin-enriched microdomains define the efficiency of native Ca^{2+}-triggered membrane fusion. *J Cell Sci,* **119,** 2688-2694.

Ruvolo, P. P. (2003) Intracellular signal transduction pathways activated by ceramide and its metabolites. *Pharmacol Res,* **47,** 383-392.

Scepek, S., Coorssen, J. R. and Lindau, M. (1998) Fusion pore expansion in horse eosinophils is modulated by Ca^{2+} and protein kinase C via distinct mechanisms. *EMBO J,* **17,** 4340-4345.

Singh, I. and Kishimoto, Y. (1983) Effect of cyclodextrins on the solubilization of lignoceric acid, ceramide, and cerebroside, and on the enzymatic reactions involving these compounds. *J Lipid Res,* **24,** 662-665.

Sot, J., Aranda, F. J., Collado, M. I., Goni, F. M. and Alonso, A. (2005) Different effects of long- and short-chain ceramides on the gel-fluid and lamellar-hexagonal transitions of phospholipids: a calorimetric, NMR, and x-ray diffraction study. *Biophys J,* **88,** 3368-3380.

Subbaiah, P. V., Billington, S. J., Jost, B. H., Songer, J. G. and Lange, Y. (2003) Sphingomyelinase D, a novel probe for cellular sphingomyelin: effects on cholesterol homeostasis in human skin fibroblasts. *J Lipid Res,* **44,** 1574-1580.

Sugita, S. (2008) Mechanisms of exocytosis. *Acta Physiol (Oxf),* **192,** 185-193.

Tamura, H., Tameishi, K., Yamagata, H., Udaka, S., Kobayashi, T., Tomita, M. and Ikezawa, H. (1992) Mass production of sphingomyelinase of Bacillus cereus by a protein-hyperproducing strain, Bacillus brevis 47, and its purification. *J Biochem,* **112,** 488-491.

Tang, K. S., Wang, N., Tse, A. and Tse, F. W. (2007) Influence of quantal size and cAMP on the kinetics of quantal catecholamine release from rat chromaffin cells. *Biophys J,* **92,** 2735-2746.

Tepper, A. D., Ruurs, P., Wiedmer, T., Sims, P. J., Borst, J. and van Blitterswijk, W. J. (2000) Sphingomyelin hydrolysis to ceramide during the execution phase of apoptosis results from phospholipid scrambling and alters cell-surface morphology. *J Cell Biol,* **150,** 155-164.

Wang, N., Kwan, C., Gong, X., de Chaves, E. P., Tse, A. and Tse, F. W. (2010) Influence of cholesterol on catecholamine release from the fusion pore of large dense core chromaffin granules. *J Neurosci,* **30,** 3904-3911.

Zidovetzki, R. and Levitan, I. (2007) Use of cyclodextrins to manipulate plasma membrane cholesterol content: evidence, misconceptions and control strategies. *Biochim Biophys Acta,* **1768,** 1311-1324.